DANMARKS OG GRØNLANDS GEOLOGISKE UNDERSØGELSE **RAPPORT 2020/29**

Capture, Storage and Use of CO_2 (CCUS)

Reservoir characterisation and hydrogeochemical reactions between CO_2 and reservoir rock

Hanne D. Holmslykke, Mette Olivarius, Claus Kjøller
& Knud Dideriksen

GEOLOGICAL SURVEY OF DENMARK AND GREENLAND
DANISH MINISTRY OF CLIMATE, ENERGY AND UTILITIES

G E U S

DANMARKS OG GRØNLANDS GEOLOGISKE UNDERSØGELSE **RAPPORT 2020/29**

Capture, Storage and Use of CO_2 (CCUS)

Reservoir characterisation and hydrogeochemical reactions between CO_2 and reservoir rock

Hanne D. Holmslykke, Mette Olivarius, Claus Kjøller & Knud Dideriksen

GEOLOGICAL SURVEY OF DENMARK AND GREENLAND
DANISH MINISTRY OF CLIMATE, ENERGY AND UTILITIES

G E U S

PREFACE

Late 2019, GEUS was asked to lead research initiatives in 2020 related to technical barriers for Carbon Capture, Storage and Usage (CCUS) in Denmark and to contribute to establishment of a technical basis for opportunities for CCUS in Denmark. The task encompasses (1) the technical potential for the development of cost-effective CO_2 capture technologies, (2) the potentials for both temporary and permanent storage of CO_2 in the Danish subsurface, (3) mapping of transport options between point sources and usage locations or storage sites, and (4) the CO_2 usage potentials, including business case for converting CO_2 to synthetic fuel production (PtX). The overall aim of the research is to contribute to the establishment of a Danish CCUS research centre and the basis for 1-2 large-scale demonstration plants in Denmark.

The present report forms part of Work package 5 and focuses on a description of the reservoir quality and properties at the Hanstholm and Havnsø structures, and on potential geochemical reactions between CO_2 and reservoir rock minerals.

Content

Dansk resumé

For at opfylde de globale mål om at begrænse CO_2-udledningen til atmosfæren er interessen vokset for geologisk lagring og udnyttelse af CO_2 i såvel Danmark som udlandet. Således er blandt andet Hanstholm- og Havnsø-strukturerne blevet identificeret som potentielle steder til CO_2-lagring. I denne rapport beskrives reservoirets egenskaber og mineralogi, og den nyeste viden om potentielle geokemiske reaktioner mellem CO_2 og sandsten gennemgås. Dette leder hen til en række forslag til mulige anbefalinger med henblik på at øge vores mineralogiske og hydrogeokemiske viden i relation til et muligt fremtidigt lagerkompleks ved Hanstholm eller Havnsø.

Den operationelle succes og den samlede lagringssikkerhed i et CO_2-lagringsprojekt afhænger i vid udstrækning af mobiliteten af CO_2 i reservoiret og dets kemiske interaktion med formationsvand og reservoirsten. CO_2 injiceret i et reservoir kan immobiliseres ved hjælp af følgende mekanismer: 1) strukturel og stratigrafisk fangst i en geologisk struktur, 2) residual fangst som bobler i porer, 3) opløselighedsfangst ved opløsning i formationsvand og 4) mineralfangst hvorved CO_2 indbygges i mineraler via kemisk udfældning. Af disse er kemiske reaktioner primært vigtige for de to sidstnævnte fangstmekanismer og har derfor betydelig indvirkning på lagringssikkerheden på længere sigt. På kortere sigt kan kemiske reaktioner nær injektionsboringen have indflydelse på injektiviteten og dermed på om et CO_2-lagringsprojekt gennemføres succesfuldt. Omfanget og hastigheden af de kemiske reaktioner er stærkt afhængige af lokale forhold såsom reservoirmineralogi, formationsvandskemi, temperatur og tryk, og stedsspecifik hydrogeokemisk viden er derfor essentiel inden opstart af et geologisk lagringsprojekt.

Hanstholm- og Havnsø-strukturerne indeholder Gassum Formation sandsten forseglet af Fjerritslev Formation muddersten. Gassum Formationen er til stede i det meste af den danske undergrund med tykkelser på typisk 50-300 m og lokalt tykkere, og den forekommer på varierende dybder. I Hanstholm-strukturen findes Gassum Formationen i en dybde af ca. 800 m, og i ca. 1300 m dybde i Havnsø-strukturen. Disse dybder angiver formationens top. Selvom mineralogien i Gassum Formationen generelt er relativ velkendt, eksisterer der ingen kernede boringer i Hanstholm- og Havnsø-strukturerne, og den nuværende viden om reservoirkvalitet og -mineralogi er derfor afhængig af estimater baseret på data fra de nærmeste repræsentative boringer.

Hanstholm-strukturens mineralogi antages at være rimeligt godt estimeret ud fra den mineralogiske sammensætning af sandstenkerner fra Thisted-3 boringen placeret ca. 50 km sydøst for strukturen. Større usikkerhed er forbundet med estimatet af mineralogien i Havnsø-strukturen da den ligger i en overgangszone, hvor data fra Stenlille boringerne placeret ca. 30 km sydøst for strukturen anvendes, da de er de nærmeste og sandsynligvis mest repræsentative. Havnsø-strukturen ligger dog mellem en kendt moden mineralogisk sammensætning på Sjælland og en mere umoden sammensætning i Jylland, og da det ikke vides hvor og hvordan ændringen i den mineralogiske modenhed sker, er den forventede mineralogi af Havnsø-strukturen baseret på den antagelse, at Havnsø har størst lighed med den østlige del af Danmark. Selvom indholdet af reaktive faser med hensyn til mineralbinding af CO_2 er højere i Jylland end på Sjælland, anses reaktionspotentialet stadig for relativt lavt baseret på den formodede mineralogiske sammensætning af sedimenterne.

Ren og tør CO_2 er ikke reaktivt, men CO_2 der injiceres i et reservoir, opløses i formationsvandet, hvilket resulterer i et fald i formationsvandets pH. Dette forskyder den oprindelige ligevægt i reservoiret, så formationsvandet bliver undermættet i forhold til mange af mineralerne i reservoiret, herunder alle metaloxider, karbonater, sulfider og multi-oxidsilikater (dvs. $A_xSi_yO_z$, hvor A repræsenterer kationer forskellige fra Si og x, y og z, støkiometriske koefficienter). Den hastighed, hvormed mineralerne opløses, varierer dog meget. For eksempel reagerer evaporitter (vandopløselige mineraler udfældet som følge af fordampning fra en vandig opløsning) hurtigt, mens silikatmineraler typisk reagerer langsommere. For mange mineraler stiger reaktionshastigheden med faldende pH, og forsuring forårsaget af CO_2-opløsning rykker derfor ikke kun opløsningen væk fra ligevægt i forhold til mineralerne, men øger også reaktionshastigheden.

Ved injektion af superkritisk CO_2 i et reservoir vil CO_2'en fortrænge det meste vand i zonen tættest på injektionsboringen. I denne relativt tørre zone er kemiske reaktioner begrænset på grund af den manglende eller meget begrænsede tilstedeværelse af vand. Eventuelt vand fanget i porerne vil opløses i CO_2'en, og denne udtørring kan medføre saltudfældning, som kan forringe porøsitet og permeabilitet i zonen nær injektionsboringen. På trods af risikoen for saltudfældning anses udtørring dog at øge den effektive CO_2-permeabilitet på grund af fjernelse af formationsvand, og udtørring forventes derfor ikke at have en væsentlig indvirkning i meget porøse og permeable sandsten som eksempelvis i Gassum Formationen.

For at undersøge om mineralopløsnings- og udfældningsreaktioner forårsaget af CO_2-injektion i Gassum Formationen påvirker reservoiregenskaberne, er der opstillet en 1D-reaktiv transportmodel med det geokemiske simuleringsværksøj PHREEQC og dets oprindelige database. I første omgang er den diffusive transport af vandige komponenter samt de kemiske reaktioner, der forventes at ske i en 2 meters zone af formationsvand nærmest en stillestående grænseflade mellem våd CO_2 og en vandmættet zone. Beregningerne indikerer, at en front med formationsvand med lavt pH spreder sig fra CO_2 / vandgrænsefladen ind i den vandfyldte zone, hvilket resulterer i opløsning af kalcit ved grænsefladen mellem det våde CO_2 og den vandmættede zone. Længere væk fra grænsefladen sker en omdannelse af silikat (i vores beregninger oligoclase) med kalcit, amorf silica og kaolinit. De geokemiske reaktioner og dermed ændringer i reservoiregenskaberne er dog ifølge modelberegningerne små, så længe vandgennemstrømningen er ubetydelig, og diffusion er den eneste betydningsfulde transportproces. Hvis den injicerede CO_2 indeholder urenheder som H_2, N_2, Ar, O_2, H_2S, CH_4, SOx og NOx, vil dette medføre yderligere forsuring, hvilket øger risikoen for ugunstige ændringer i reservoiregenskaberne i nærheden af injektionsboringen væsentligt. Vi anbefaler, at systemet studeres yderligere gennem mere detaljeret modellering og muligvis laboratorieeksperimenter.

Opløsningen af eksempelvis kalcit kan skabe små partikler i reservoiret, såkaldte fines. Efterhånden som injektionen af CO_2 fortsætter, og grænsefladen mellem CO_2 og formationsvand passerer over de genererede fines, kan disse fines mobiliseres og potentielt tilstoppe pore-halsene, hvilket resulterer i reduceret injektionsevne. Under injektionsstop kan trykgradienten i reservoiret midlertidigt vendes, hvilket fører eventuelle mobiliserede fines mod injektionsboringen, hvilket øger risikoen for nedsat injektionsevne. Potentialet for mobilisering af fines i Gassum Formationen på grund af injektion af CO_2 er dog ukendt, og laboratorieeksperimenter til afklaring af dette anbefales.

Da densiteten af den injicerede CO_2 er lavere end formationsvandets, bevæger CO_2 sig opad i reservoiret og akkumuleres i toppen af reservoiret lige under det uigennemtrængelige segl. Opløsning af CO_2 i formationsvandet resulterer i en stigning i densiteten af formationsvandet, som med tiden kan føre til en nedadgående densitet-styret transport af CO_2-beriget formationsvand. 1D reaktiv transportmodel-beregninger med strømning af CO_2-holdigt vand gennem Gassum Formationen indikerer, at densitetsdrevet strømning kan resultere i betydelig omdannelse af silikater til karbonater, hvis strømningshastigheden er langsom. Således indikerer beregningerne, at for en CO_2-plume, der dækker 1 km^2 med densitetsdrevet strømning, vil potentielt ca. 0,6 Mton CO_2 være fanget ved opløsning i formationsvandet, mens 0,4 Mton potentielt vil være fanget ved indbygning i mineraler via kemisk udfældning. Disse beregninger involverer flere forsimplinger og antagelser, herunder en gennemsnitlig mineralogiske sammensætning af reservoiret, og resultaterne giver kun et grundlæggende indtryk af de tidsskalaer, hvorved fangst kan forekomme, når der tages hensyn til mineralreaktionshastigheder. I betragtning af vigtigheden af den tidsmæssige udvikling af CO_2-fangstmekanismer i forbindelse med CO_2 lagring anbefales yderligere undersøgelser for at belyse fangstpotentialet i Hanstholm- og Havnsø-strukturerne.

Anbefalinger til fremtidige undersøgelser

Det anbefales at etablere en diagenesemodel for geologiske strukturer, der overvejes at blive anvendt til CO_2-lagring. Dette bør gøres for at estimere den mineralogiske sammensætning, der er relevant for reservoirets reaktivitet, og for at estimere porøsitet og permeabilitet der er essentielle for reservoirets ydeevne. Nye laboratorieanalyser og metodeudvikling anbefales i forbindelse med at forbedre de prædiktive modeller således at mineralogi og reservoiregenskaber vil kunne blive estimeret tilfredsstillende godt for hele reservoiret.

For at øge vores forståelse af de specifikke hydrogeokemiske reaktioner mellem CO_2 og reservoiret i henholdsvis Hanstholm- og Havnsø-strukturen anbefales en plan med tre trin: Først udføres indledende modellering for at definere kritiske ubekendte, der skal kvantificeres eksperimentelt og danne grundlag for optimal design af laboratorieeksperimenter. Dernæst udføres laboratorieeksperimenter ved hjælp af stedspecifikt kernemateriale. Dette eksperimentelle arbejde vil give de nødvendige data til optimal modellering af de kritiske processer i det CO_2-holdige reservoir. Slutteligt foretages den endelige geokemiske modellering for at kvantificere effekten af geokemiske reaktioner på lagerenhedens ydeevne og fangstpotentiale.

Summary

To meet the global goals of restricting the CO_2 emission to the atmosphere, geological storage and utilisation has gained increased interest in Denmark as well as abroad. The Hanstholm and Havnsø structures have among others been identified as potential CO_2 storage sites. In this report, the reservoir properties and mineralogy are described together with a review of state-of-the-art knowledge of potential geochemical reactions between CO_2 and sandstones, leading to recommendation for increasing our mineralogical and hydrogeochemical knowledge coupled to a possible future Danish storage complex at Hanstholm or Havnsø.

The operational success and overall storage security of a CO_2 storage project depends to a large extend on the mobility of CO_2 in the reservoir and its chemical interactions with the formation water and reservoir rock. CO_2 injected into a reservoir may be immobilized by one of the following mechanisms 1) structural and stratigraphic trapping in a geological structure, 2) residual saturation trapping as bubbles in pores, 3) solubility trapping by dissolution in formation water, and 4) mineral trapping by which CO_2 is incorporated into minerals due to chemical precipitation. Of these, chemical reactions are important mainly for the latter two trapping mechanisms and therefore have a significant impact for storage security over longer time scales. At shorter time scales, chemical reactions near the injection well may have an impact on the injection operation and as such determine the success of a CO_2 storage project. For example, mineral dissolution is expected to increase porosity and permeability and thereby increase storage capacity and injectivity. Dissolution of minerals may, however, also be critical to the mechanical strength of the reservoir. Mineral precipitation on the other hand may decrease the porosity and permeability which may under certain conditions reduce injectivity. The extent and rate of these chemical reactions are highly dependent on local conditions such as reservoir mineralogy, formation water chemistry, reservoir temperature and pressure, etc. Therefore, site specific hydrogeochemical knowledge and investigations are essential prior to any geological storage project.

The Hanstholm and Havnsø structures contain Gassum Formation sandstones sealed by Fjerritslev Formation mudstones. The Gassum Formation is present in most of the Danish subsurface with thicknesses of mostly 50–300 m and locally thicker, and it occurs at depths ranging from more than 3 km in the basin centre in central Jutland to less than 1 km near the basin margins to the north and south. In the Hanstholm structure, the Gassum Formation has a top point at c. 800 m and a spill point at c. 1000, whereas the Havnsø structure has top point at c. 1300 m and spill point at c. 1600 m. Although the Gassum Formation in general is relatively well characterised, no cored wells exist for the Hanstholm and Havnsø structures and thus our present knowledge of the Gassum Formation at the two structures rely on estimates based on data from the nearest representative offset wells. The reservoir quality at Hanstholm and Havnsø is estimated from porosity and permeability data from wells in Thisted (*c.* 50 km away from the structure) and Stenlille (*c.* 30 km away from the structure), respectively, where the reservoir quality is found to be sufficiently good for CO_2 storage.

The mineralogy of the Hanstholm structure is expected to be reasonably well estimated from the mineralogical composition of the fluvial, estuarine, lagoonal and shoreface sandstone

cores from the Thisted-3 well located c. 50 km southeast of the structure. Thus, in average, the sandstones are expected to be dominated by quartz (62%) with significant contributions of plagioclase (10%), K-feldspar (8%) and detrital clays (8%) and minor amounts (< 2%) of mica minerals, rock fragments, heavy metals, authigenic kaolinite, calcite, ankerite, siderite and pyrite, although the carbonate minerals could potentially be present in significant amounts in some intervals. Larger uncertainty is related to the estimate of the mineralogy of the Havnsø structure, since it is situated in a transition zone that is not well understood. Data from the Stenlille wells located c. 30 km southeast of the structure are used since they are the nearest and probably the most representative. The Havnsø structure is located between a known mature mineralogical composition with high quartz content in Zealand and a more immature composition with more feldspars, micas, rock fragments and heavy minerals in Jutland. Since it is unknown where and how the change between mature mineralogy to the east and immature mineralogy to the west occurs, the expected mineralogy of the Havnsø structure is based on the assumption that Havnsø has resemblance to the eastern part of Denmark. The sandstone in the Havnsø structure is thus estimated to be dominated by quartz (86%), with small contributions of detrital clays (4%), K-feldspar (3%), authigenic kaolinite (2%), plagioclase (1%), rock fragments (1%) and calcite/ankerite (1%), though the carbonate minerals may in some intervals occur in large amounts. Although the content of reactive phases with regards to mineral sequestration of CO_2 in the Gassum Formation such as albite, oligoclase and chlorite is higher in Jutland than in Zealand, the reaction potential is still considered relatively small based on the assumed mineralogical composition of the sediments.

Pure and dry CO_2 is not reactive. CO_2 injected into a reservoir will, however, dissolve in the formation water resulting in a decrease in the pH of the formation water. This shifts the original equilibrium in the reservoir, so the formation water becomes subsaturated with respect to many of the minerals in the reservoir, including all metal oxides, carbonates, sulphides and multioxide silicates (i.e., $A_xSi_yO_z$, where A represents cations different from Si and x, y and z, stoichiometric coefficients). The rate by which the minerals dissolve varies, however, greatly. For example, evaporite minerals react fast, while silicate minerals typically react more sluggishly. For many minerals, reaction rates increase with decreasing pH, and the acidification caused by CO_2 dissolution therefore not only shifts the solution away from equilibrium with respect to the minerals, it also increases the mineral reaction rates.

As supercritical CO_2 is injected into the reservoir, it displaces most of the water in the zone closest to the injection well. Some residual water will, however, be trapped in pore spaces because of surface tension. In this relatively dry zone chemical reactions are limited because water is absent or present in low concentration in the CO_2. Dissolution of water in the CO_2 will remove the residual water closest to the well and this desiccation could cause salt precipitation which may impair porosity and permeability in the zone near the injector well. Despite the risk of salt precipitation, the desiccation is believed to increase the effective CO_2 permeability due to the removal of formation water and desiccation is therefore not expected to have a major impact in highly porous and permeable sandstones such as the Gassum Formation sandstones.

To evaluate if mineral dissolution and precipitation reactions caused by CO_2 injection into the Gassum Formation affect the reservoir properties, 1D reactive transport modelling with the geochemical software PHREEQC and its native database has been applied. First, the diffusive transport of aqueous species and the mineral reactions occurring in a 2 m zone of formation water closest to a stagnant interface between wet CO_2 and a completely water saturated zone has been modelled. The calculations indicate that a low pH front propagates from the CO_2/water interface into the sediment which causes some calcite to dissolve at the wet CO_2/water saturated zone interface. Further away from the interface, silicate (in our calculations oligoclase) is replaced by calcite, amorphous silica and kaolinite. Geochemical reactions are, however, minor and consequently alterations to the rock will according to the model be fairly small as long as water flow is negligible, and diffusion is the only transport process that operates. If the injected CO_2 contains impurities such as H_2, N_2, Ar, O_2, H_2S, CH_4, SO_x and NO_x this will cause additional acidification, which will substantially increase the risk for adverse changes to the rock properties in the vicinity of the injection well. We recommend that the system be studied further through more detailed modelling and laboratory experiments.

The dissolution of inter-granular cement such as calcite may create fine particles. As CO_2 injection continues and the CO_2/formation water interface passes over the generated fines, the fines may be mobilized and may potentially clog the pore throats resulting in reduced injectivity. During injection stops, the pressure gradient in the reservoir may temporarily be reversed, leading any mobilized fines towards the injection well, and thereby increasing the risk of reduced injectivity. The potential for fines migration in the Gassum formation due to CO_2 injection remains unknown, and laboratory experiments to clarify this are recommended.

Since the density of the injected CO_2 is lower than that of the formation water, the CO_2 will move upwards in the reservoir and accumulate in the top of the reservoir just below the impermeable cap rock. Dissolution of CO_2 in the formation water results in an increase in the density of the formation water which with time may lead to a density driven downwards transport of CO_2 enriched formation water. 1D reactive transport calculations with flow of CO_2 charged water through the Gassum Formation indicate that density driven flow may result in substantial silicate carbonation if the flow velocity is slow. Thus, the calculations indicate that for a CO_2 plume covering 1 km^2 with density driven flow, c. 0.6 Mton of CO_2 may be solubility trapped while 0.4 Mton may be mineral trapped after 4,000 years. These calculations involve several simplifications and assumptions, including an averaged rock composition for the Gassum Formation, and the results merely provide a basic impression of the time scales at which trapping may occur, when mineral reaction rates are taken into account. Given the importance of the evolution of CO_2 trapping mechanisms with time, additional work to elucidate the trapping potential in the Hanstholm and Havnsø structures is recommended.

Recommendations for future research

The establishment of diagenesis models is recommended for geological structures considered for CO_2 storage to estimate the mineralogical composition relevant for reservoir reactivity and to estimate the porosity and permeability that are essential for reservoir performance. Input to the models must include data from existing wells, and site-specific assumptions must be made regarding the burial history and depositional environments on the relevant locations. Such models could optimally be extended across the entire geographical distribution of each reservoir based on basin-wide sequence stratigraphic correlations and seismic mapping. Development of a machine learning approach in the mineralogical quantification of detrital and authigenic phases is recommended since such an automated procedure will include mineral chemistry and remove operator bias.

To increase our understanding of the specific hydrogeochemical reactions between CO_2 and reservoir minerals in the Hanstholm and Havnsø structures, respectively, a three stage plan has been proposed: Firstly, preliminary modelling is performed to define critical unknowns that should be quantified experimentally and provide the basis for design of the laboratory experiments. Secondly, laboratory experiments are carried out using site specific core material. This experimental work will provide information required for optimal modelling of the critical processes in the CO_2 containing reservoir. Thirdly, the final geochemical modelling to quantify the impact of geochemical reactions on the performance of the storage facility.

1. Introduction

The growing concern of global warming caused by large CO_2 emission to the atmosphere due to combustion of fossil fuels has increased the focus on geological storage and utilization of CO_2 as possible mitigation measures for reducing the emission to the atmosphere. Several potential CO_2 storage sites have been identified in the sandstone reservoirs in the deep subsurface onshore and nearshore Denmark. Two of these are the Hanstholm and Havnsø structures, both of which contain Gassum Formation sandstones sealed by Fjerritslev Formation mudstones.

This report focuses on a description of the reservoir quality and properties at the Hanstholm and Havnsø structures, and on potential geochemical reactions between CO_2 and reservoir rock minerals. The fate of CO_2 in the reservoir is highly dependent on local chemical reactions taking place over the entire time scale of a CO_2 storage and utilization project. Therefore, hydrogeochemical knowledge and research on a local scale is a vital part of any such project, ranging from collection of specific hard data to predictions made by numerical modelling. Therefore, this report provides a description of state-of-the-art knowledge of potential reactions between CO_2 and sandstones and possible ways to establish hydrogeochemical knowledge for a future Danish storage complex at Havnsø or Hanstholm.

2. Reservoir quality and properties

2.1. Reservoirs relevant for CO_2 sequestration

Reservoirs applicable for subsurface CO_2 storage consist of porous rocks such as sand and sandstone where it is possible to store large volumes of CO_2. High permeability is required so that CO_2 can be dispersed quickly in the reservoir after injection. For CO_2 storage and utilization projects, the reservoir must be positioned deeper than c. 800 m so that the CO_2 is supercritical ($scCO_2$). In its supercritical state, the CO_2 will act like a gas and thus expand to fill out the available space while having a density like that of a liquid. The density of the formation water is, however, larger, meaning that $scCO_2$ will move upwards in the reservoir. Thus, storage of CO_2 requires that a seal is present above the reservoir to prevent leakage. Preferably, the seal forms an upwards-closed structure into which the CO_2 can be injected such that its distribution is controlled by this trap.

The amount of CO_2 that can be stored depends on the size of the structure, the depth, the reservoir properties, the chemical composition of the formation water and the mineralogy of the reservoir rocks. CO_2 injected into a reservoir can be sequestered by several immobilization mechanisms such as structural and stratigraphical trapping in a geological structure, residual saturation trapping as bubbles in pores, solubility trapping by dissolution in formation water, and mineral trapping though formation of carbonates (See section 3 for details) (Bachu, 2003; Bachu and Adams, 2003; Burnside and Naylor, 2014; Sundal and Hellevang, 2019).

For a CO_2 storage reservoir, the reactivity of the rock must be considered since the CO_2 may induce dissolution and precipitation of minerals in the reservoir, which may be either a benefit or a disadvantage depending on the circumstances. Mineralization of the injected CO_2 can be an advantage to ensure long-term storage, especially in reservoirs with open boundaries where immobilization of the plume cannot be achieved by the caprock alone (Olivarius et al., 2019a) or in permeable basaltic rocks where the CO_2 can react with the volcanic material and form carbonate minerals (Oelkers et al., 2008; Matter et al., 2016). However, the mineralization must not occur too close to the wellbore since this could reduce injectivity and the minerals in the reservoir must not be dissolved so much that the reservoir starts compacting.

2.2. Potential CO_2 storage reservoirs in Denmark

In most parts of onshore Denmark, one or several potential CO_2 storage reservoirs are present in the subsurface outside the areas with shallow basement, which include parts of the Ringkøbing–Fyn High, Bornholm and northernmost Jutland. In parts of central and northern Jutland and northern Zealand, the deepest sandstones are too tight for storage so shallower reservoir sandstones may be used instead (Vosgerau et al., 2016). In areas containing potential reservoirs, relevant geological structures can then be investigated in detail to determine their trapping ability. Many potential storage structures have been identified in the

Danish area for which the suitability can be determined by further investigations (Fig. 2.1) (Anthonsen et al., 2011).

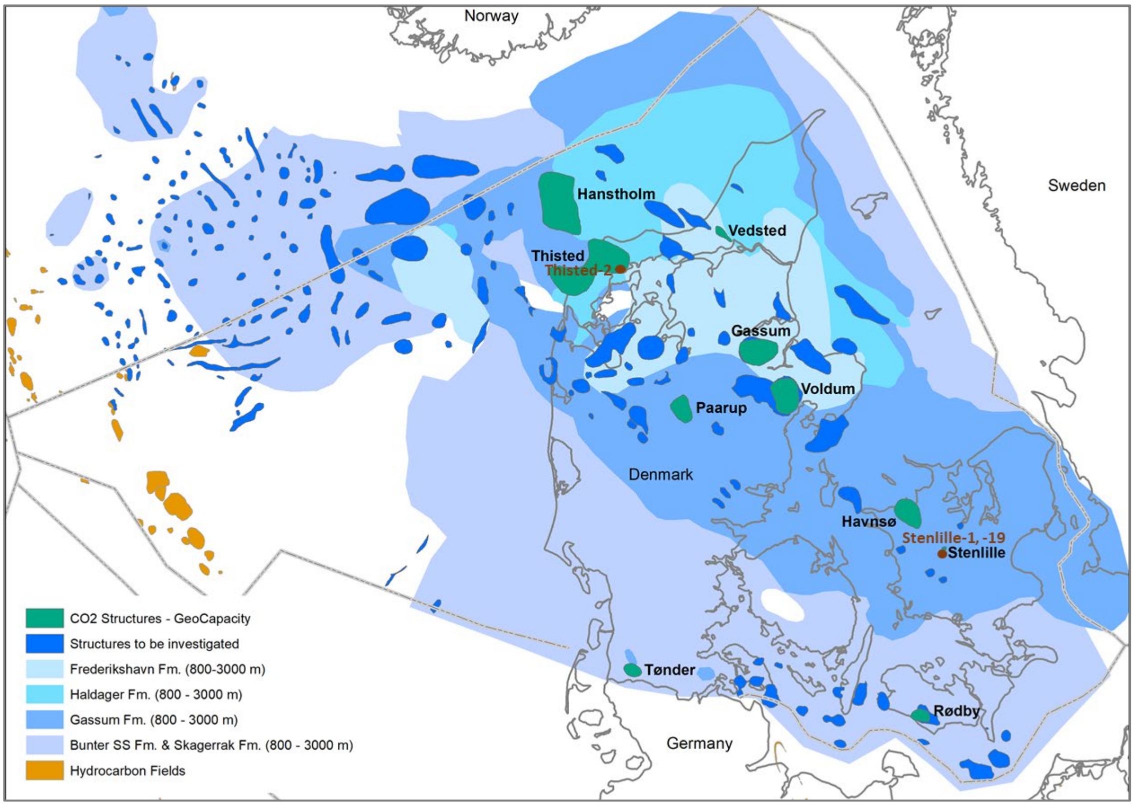

Figure 2.1. Map from Anthonsen et al. (2011) of the Danish area showing the distribution of sandstone formations (Fm) with potential for CO_2 storage and the structures that may be used as traps for the injected CO_2. The structures named Hanstholm and Havnsø with reservoir in the Gassum Formation are the focus of this report. No storage potential occurs on Bornholm due to the shallow position of the basement. The figure includes wells penetrating the Gassum Formation from which formation water chemistry data are available (Laier, 2008).

The reservoirs applicable for CO_2 storage comprise onshore Mesozoic sandstone layers that are also relevant for exploitation of geothermal energy, and the reservoirs have been targets of partly successful geothermal exploration and unsuccessful oil/gas exploration. Thus, much knowledge of these sandstones has been obtained from analyses of core and water samples, wireline logs and seismic mapping. The reservoir properties, brine composition, mineralogy, diagenesis, provenance, sedimentology and stratigraphy of the sandstones have recently been revisited in a geothermal context (e.g. Hjuler et al., 2014; Kristensen et al., 2016; Vosgerau et al., 2016a, 2017; Weibel et al., 2017a, 2017b; Erlström et al., 2018; Olivarius et al., 2018a; Holmslykke et al., 2019a, 2019b; Kazmierczak et al., 2019; Olivarius et al., 2019b, 2020a; Weibel et al., 2020). Additionally, mapping of reservoir depth, thickness, temperature and geothermal resource has been performed (Vosgerau et al., 2016b; Fuchs et al., 2020; Mathiesen et al., 2020b), with results presented in the online application "Geotermi WebGIS-portalen".

The primary geological formations with potential reservoir rocks for onshore CO_2 storage in Denmark comprise the Lower Triassic Bunter Sandstone Formation, the Lower to Upper Triassic Skagerrak Formation, the Upper Triassic to Lower Jurassic Gassum Formation and the

Middle Jurassic Haldager Sand Formation (Fig. 2.1). All these formations contain permeable sandstone intervals (Weibel et al., 2020); however, the depth and extent of each reservoir vary considerably across the country due to their different depositional regimes and the post-depositional structural inversion events with associated erosion (Nielsen, 2003; Japsen et al., 2007). This results in variable reservoir quality. Some formations of more local occurrence may also contain sandstones appropriate for CO_2 storage. These include the Upper Jurassic Flyvbjerg Formation, the Upper Jurassic to Lower Cretaceous Frederikshavn Formation, and unnamed sandstone intervals in the Lower Jurassic Fjerritslev Formation and in the Lower Cretaceous deposits.

The Gassum Formation is used for storage of natural gas in the Stenlille structure (Laier and Øbro, 2009), for geothermal energy for district heating in Sønderborg and Thisted (Mathiesen et al., 2020b), and the formation also has potential for heat storage (Rosenbrand et al., 2014; Holmslykke et al., 2017; Major et al., 2018; Pasquinelli et al., 2020). These different utilization options may in the coming years lead to the necessity of an integrated areal management such that the subsurface may be optimally used for the various storage and energy extraction purposes. Among these, CO_2 storage is considered important to be able to meet the goals of reduced greenhouse gas emission (Metz et al., 2005). Some synergies between the different green utilizations of the subsurface may be possible such as CO_2 storage combined with reinjection of water used for geothermal heat extraction (Mathiesen et al., 2003). The evolving Power-to-X technologies may make it possible to reuse stored CO_2 in the future in integrated smart energy systems (Mathiesen et al., 2015; Lund et al., 2016; Eveloy and Gebreegziabher, 2018; Anthonsen et al., 2019).

2.3. Risks management

Several risk elements must be considered in relation to subsurface CO_2 storage (Jakobsen, 2020; Keiding, 2020; Larsen et al., 2020). Modelling of the reactions that may occur between the injected CO_2 and the reservoir rocks is important to predict possible changes in injectivity and rock strength. The risk of leakage of CO_2 along natural faults that may crosscut the sealing rocks can be estimated via seismic data comprising preferably a 3D survey of the structure considered for injection. Potential micro-seismicity induced by injection can be monitored during storage and the baselevel of natural activity must be measured prior to injection. The risk of formation damage is important to consider since fines migration and clay swelling may be triggered if drilling fluids intrude in clayey sandstones, resulting in decreased permeability near the injection well such that the amount of CO_2 that can be injected is reduced. The public perception of CO_2 storage projects must be considered where for example public meetings for the local communities near potential storage sites may be fruitful to generate a high information level and promote constructive communication concerning potential risks associated with subsurface CO_2 storage.

2.4. Geological setting of Gassum Formation

The Gassum Formation was defined by Larsen (1966) for the Danish area and later redefined by Bertelsen (1978). The sedimentology, stratigraphy and distribution were described in more detail by Michelsen et al. (2003) and Nielsen (2003). The Gassum Formation occurs mainly in the Norwegian–Danish Basin and is locally present in the North German Basin. The basins were formed during regional subsidence after rifting phases (Vejbæk, 1997). These basins are divided by the Ringkøbing–Fyn High, which is a basement high that crosscuts the Danish area in an east-west direction on which only thin sediment packages could accumulate.

The Gassum Formation typically has thicknesses of 50–300 m. It is locally thicker, especially in the Sorgenfrei–Tornquist Zone (Nielsen and Japsen, 1991; Michelsen et al., 2003; Nielsen, 2003; Mathiesen et al. 2020b). The deposition took place during repeated sea-level fluctuations where fluvial and shoreface sand was deposited during regression and interbedded with marine and lacustrine mud during transgressions. The fluvial sand was deposited by braided streams, followed by estuarine and lagoonal sand deposition near the sea, and shoreface sand was deposited as lateral continuous bodies along the coastline (Nielsen, 2003).

The depth of the Gassum Formation varies greatly across Denmark with largest depths of >3 km occurring in the basin centre (i.e. central Jutland) and smallest depths of <1 km near the basin margins to the north and south. The present-day burial depths are shallower than the maximum burial depths that the formation has experienced prior to uplift events, of which the largest regional inversion occurred during the Neogene (Japsen and Bidstrup, 1999; Nielsen, 2003; Japsen et al., 2007). This resulted in substantial erosion in differential amount, increasing in magnitude towards the northeast. The amount of uplift is estimated from sonic velocities, vitrinite reflectance, apatite fission-track analyses and mineralogical temperature indicators (Japsen et al., 2007; Petersen et al., 2008; Weibel et al., 2017b).

Salt tectonics with movement of the Zechstein deposits and hence also the overlying formations has caused local variations in the depth of the Gassum Formation, especially in central Jutland, and positive temperature anomalies occur within a few kilometers' distance of the salt structures (Vejbæk, 1997; Fuchs et al., 2020). The geothermal gradient i.e. the temperature-depth gradient in the subsurface is 25-30°C/km in Denmark, locally up to 35°C/km (Fuchs et al., 2020), and a temperature of 8°C is present at the surface, corresponding to varying temperatures of 30–100°C in the depth interval of 800–3000 m applicable for storage.

Many structures with CO_2 storage potential are present in the Gassum Formation (Hjelm et al., 2020) sealed by Fjerritslev Formation mudstones (Springer et al., 2020). In this report, the Hanstholm and Havnsø structures are in focus (Fig. 2.1), which both contain Gassum Formation sandstones that have been mapped through interpretation of seismic data from the two structures and from adjacent areas with better data (Gregersen et al., 2020; Rasmussen and Laghari, 2020; Vosgerau et al., 2020). The Gassum Formation in the Hanstholm structure has top point at c. 800 m depth and spill point at c. 1000 m, whereas the Havnsø structure has top point at c. 1300 m and spill point at c. 1600 m (Mathiesen et al., 2020a) (Fig. 2.2).

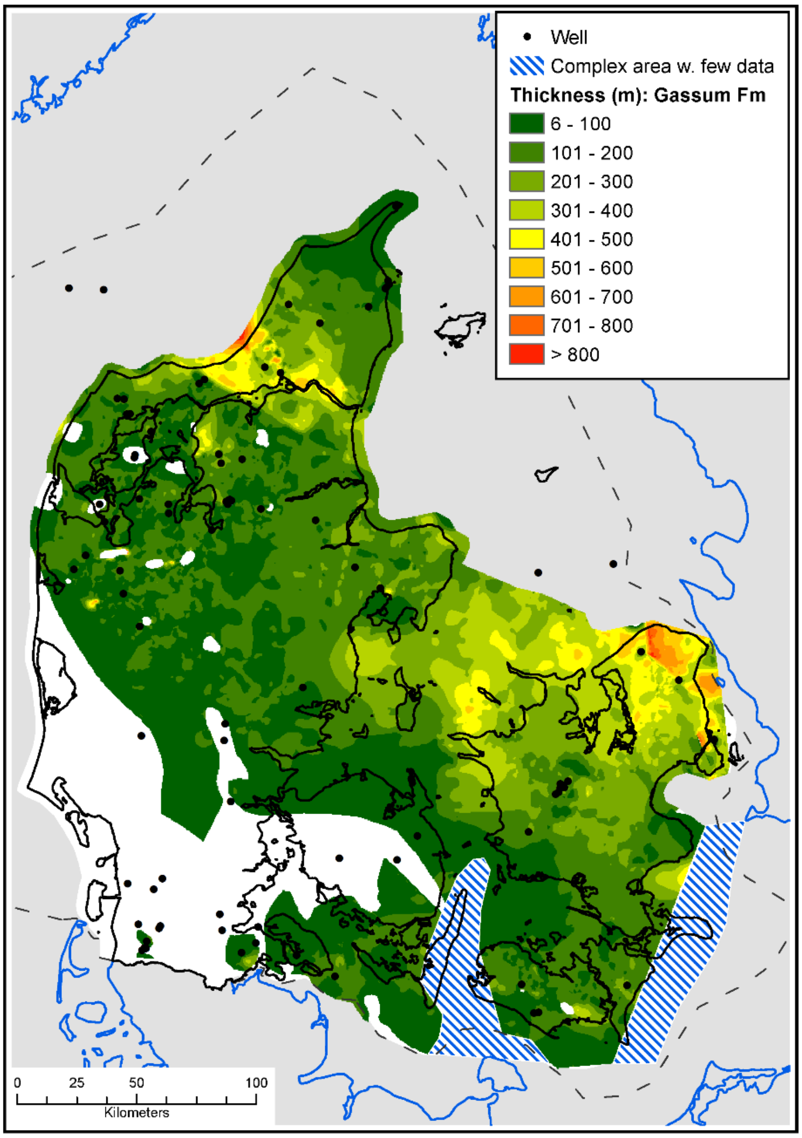

Figure 2.2. Map of the thickness of the Gassum Formation (Mathiesen et al. 2020b).

2.5. Reservoir properties of Gassum Formation

For the Danish geothermal reservoir sandstones, the potential reservoir intervals termed ‘net sand’ are defined as having a porosity above 15% and a clay content below 30% (Kristensen et al., 2016). This practice is adopted from the hydrocarbon exploration such that only intervals with sufficient capacity are included. Furthermore, a minimum transmissivity of 10 Darcy-metre is preferred for the geothermal reservoirs. A similar approach may be used to determine which reservoir intervals are appropriate for CO_2 storage or another methodology may be applied that is less dependent on permeability.

Factors that control the reservoir properties comprise grain size, clay content and diagenesis. The grain size distribution and initial mineralogical composition including clay content are determined by the depositional environment, the climatic conditions during deposition, the distance to the provenance and the composition of the sediment source rocks (e.g. Morton and Hallsworth, 1994; Nielsen, 2003; Weibel et al., 2017b). Diagenesis is the process by which sand is turned into sandstone during burial where unstable minerals dissolve at increasing temperature and new minerals precipitate between the grains thus cementing them together. Eventually, the sandstones become so tight that the porosity and permeability are too low for a reservoir rock making them inapplicable for CO_2 storage, which occurs at depths of c. 3 km in Denmark (Weibel et al., 2020). The salinity of the formation water in the Danish reservoirs increases with depth, which must be considered since the CO_2 solubility decreases correspondingly (e.g. Laier 2008; Holmslykke et al., 2019a).

Porosity and gas permeability were measured by routine core analysis (API, 1998) and grain size of the samples were measured manually. The porosity-permeability relationship of the Gassum Formation varies with grain size and cementation (Weibel et al., 2017a) with the best reservoir quality being present in the most coarse-grained sandstones with the smallest amounts of cement (Fig. 2.3A). Thus, knowledge of the depositional environments and the diagenetic development are important to make reliable pre-drill estimates of reservoir properties in undrilled areas. The depths of the samples have been recalculated to the estimated maximum burial depths prior to uplift, and the porosity and permeability show an overall decrease with depth, but varies much depending on the grain size, clay content and diagenesis (Fig. 2.3B).

Screening of the geothermal potential in 28 Danish cities with large district heating networks has previously been conducted, where the results from Thisted and Kalundborg are most representative for the Hanstholm and Havnsø localities, respectively. For Havnsø/Kalundborg, data from the Stenlille wells are considered most representative (Kristensen, 2020). The results from both cities indicate that the Gassum Formation has good reservoir quality with estimated porosity of 24–27%, gas permeability of 433–3900 mD and transmissivity of 38–342 Dm for Thisted, and porosity of 22–27%, gas permeability of 118–2944 mD and transmissivity of 15–537 Dm for Kalundborg (Vosgerau et al., 2015a, 2015b, 2016b). These estimates cannot be considered directly applicable for the storage localities in question since the depth, thickness and facies may be different, and the data used to produce the estimates are scattered. Nevertheless, the estimates for the two cities indicate that the Gassum Formation is likely to have sufficiently good reservoir quality for CO_2 storage in the Hanstholm and Havnsø structures.

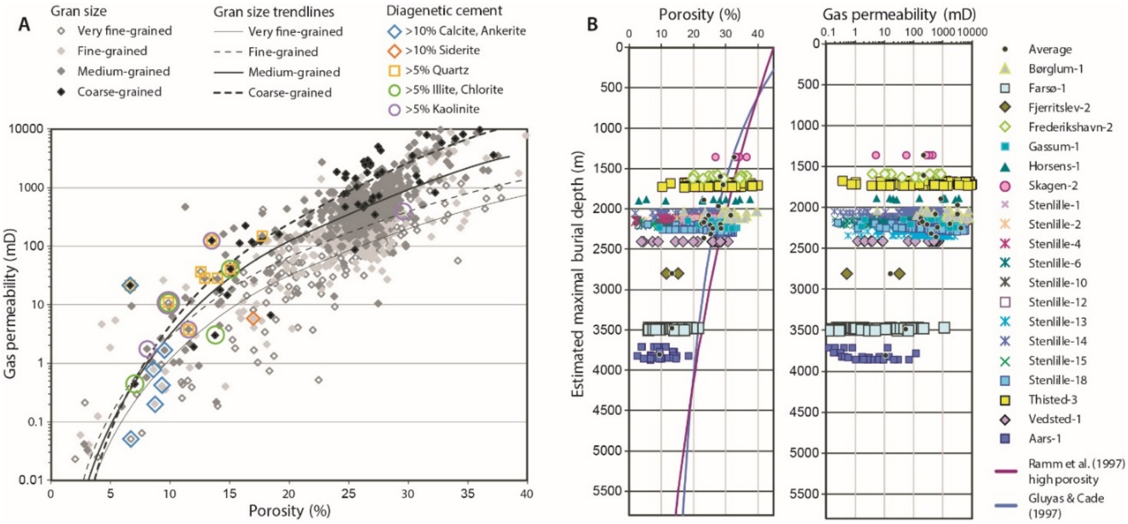

Figure 2.3. Reservoir properties of the Gassum Formation based on Weibel et al. (2020). A: The porosity-permeability relationship varies with the grain size. The primary diagenetic cement types are shown for selected samples. The best reservoir quality is present in the most coarse-grained sandstones with the lowest abundance of cement. B: The porosity and permeability show an overall decrease with depth, but varies much depending on the grain size, clay content and diagenesis. The estimated maximum burial depths are corrected for structural inversion (Japsen and Bidstrup, 1999; Japsen et al., 2007). The mechanical compaction curves are from Gluyas and Cade (1997) and Ramm et al. (1997).

2.5.1. Evaluation of data quality

The reservoir properties and mineralogical composition have been measured on sandstone cores that have in many cases been dry for years, which may have changed the morphology of authigenic clay minerals. Furthermore, salt precipitations have formed from drying of the saline pore fluids. The salt has in most cases been removed by methanol prior to analyses, but the most porous sandstones were too fragile for cleaning, so the reservoir properties of these samples are presumably underestimated. The reservoir properties of the uncemented sand intervals could not be measured, so these sands with presumed high porosity and permeability do not appear in the results. Drying and pressure release of the cores has caused micro-fracturing in some cases, which can be difficult to distinguish from natural fractures. In some cases, the plugs have cracked during permeability measurement thus increasing the measured permeability. The reservoir properties have in most cases been measured on horizontal plugs and in some cases on vertical and oblique plugs, which may cause some discrepancy. However, only horizontal plugs were used in the plots in Figure 2.3.

The permeability is measured with gas although liquid would be more accurate to mimic the reservoir conditions, so a relationship has been established to convert the measured gas permeabilities into more realistic liquid permeabilities. This gas to liquid permeability relationship is different for each sandstone formation, but in all cases the liquid permeabilities are lower than the corresponding gas permeabilities (Holmslykke et al., 2019b). Furthermore, stressed porosity and fluid permeability has been measured on a subset of samples to determine how they are influenced by reservoir pressure. The results show that the porosity decreases only slightly whereas the permeability decreases considerably with increasing pressure (Olivarius et al., 2019b).

The mineralogical composition has been determined by two different operators, which may have induced some inconsistency in the results since the optical point-counting identification of minerals is slightly subjective. Furthermore, not all minerals can be designated optically, so minor phases may have been overlooked in those samples for which the chemical composition of the minerals has not been checked by SEM-EDX. The performed grain-size analysis of thin-sections in general underestimates the grain size relative to sieving analysis (Johnson, 1994).

2.6. Mineralogy of Gassum Formation

The mineralogy, petrographic relationships, texture, grain size and sorting of the Gassum Formation sandstones were studied by transmitted and reflected light microscopy of polished thin sections including point counting to quantify the mineralogical composition. Scanning electron microscopy (SEM) including energy dispersive X-ray analysis (EDX) were applied for chemical identification of minerals and for studies of crystal morphologies and paragenetic relationships in rock-chip samples.

The detrital mineralogy is dominated by quartz with smaller amounts of K-feldspar, plagioclase, mica, clay, rock fragments and heavy minerals (Fig. 2.4). The reservoir rocks consist of loose sand in the shallowest wells whereas tight sandstones can be found in the deepest wells, so the diagenesis is important to consider (Friis 1987; Weibel 2017a, 2017b). The types of authigenic minerals that have formed in the sandstones are related to depositional environment and depth, and the amount of authigenic minerals increases in general with depth. For example, quartz cement forms continuously on quartz grains during elevated temperatures, whereas shell-lag horizons in shoreface sandstones can cause pervasive carbonate cementation already at shallow depth. The pore-filling minerals comprise primarily quartz, calcite, ankerite, siderite, kaolinite, illite, chlorite and pyrite (Fig. 2.4). The type, morphology and amount of these diagenetic minerals strongly affect the reservoir properties (Fig. 2.4).

The detrital composition is dependent om provenance where a high mineralogical maturity with high quartz content is present in Zealand, whereas a less mature composition with more feldspars, micas, rock fragments and heavy minerals is found in Jutland (Vosgerau et al., 2016a; Weibel et al., 2017a, Olivarius et al. 2020b). Although the mineralogical composition of the Gassum Formation is well-known, it is uncertain where and how the change between mature mineralogy to the east and immature mineralogy to the west occurs, so the mineralogical composition estimated for the Havnsø structure is considered less reliable than the estimate made for the Hanstholm structure due to the more central location of Havnsø. Interpretation of the distribution of depositional environments and the sediment transport directions is very important in this respect since no deep wells exist between Jutland and Zealand (Nielsen and Japsen, 1991; see GEUS Well Data Summary Sheets for newer deep wells). Provenance data indicates that the mature mineralogy is caused by sediment input to the basin from the southeast which only reached the eastern/southeastern part of Denmark, whereas less mature sediment sourced from the north/northeast spread all across the area (Weibel et al., 2017b; Olivarius et al., 2018b, 2019a, 2020b).

Based on data from the nearest wells (Japsen and Bidstrup, 1999; Japsen et al., 2007), the Neogene inversion of the Danish area is estimated to have caused uplift of c. 800 m for the Hanstholm structure and c. 600 m for the Havnsø structure. The estimate is least certain for Havnsø where no nearby wells exist and hence data from the Stenlille wells located c. 30 km southeast of the structure are used, whereas data from the Felicia-1 and J-1 wells are used for Hanstholm, of which Felicia-1 is located on the eastern rim of the structure and J-1 is positioned c. 15 km further to the east. Considering the present-day depths corrected for uplift, this corresponds to estimated maximum burial depths of the Gassum Formation of c. 1600-1800 m in Hanstholm and c. 1900-2200 m in Havnsø, taken from top point to spill point of the structures.

These maximum burial depths are important since the amount of diagenesis is determined by the maximum temperature and pressure that the sandstones have been exposed to. These depths correspond to temperatures of less than 80°C meaning that the reaction potential with CO_2 is small (Olivarius et al., 2019a). This was also shown by core experiments with CO_2 injection in Gassum Formation sandstones at 70°C and 20 MPa where only carbonate minerals notably reacted (Weibel et al., 2014). Although the content of reactive phases with regards to mineral sequestration of CO_2 in the Gassum Formation such as albite, oligoclase and chlorite is higher in Jutland than in Zealand, still the reaction potential is relatively small as a result of the mineralogical composition of the sediments (Weibel et al., 2017a, 2017b).

In the Gassum Formation, ankerite replaces calcite with depth (Weibel et al., 2017a), which in general decreases the reservoir quality since the ankerite is often pervasive. The replacement seems to happen around 2000–2300 m maximum burial depth, meaning that both minerals may occur in the Hanstholm and Havnsø structures, and both minerals have indeed been found in sidewall cores from the J-1 well (Olivarius et al., 2019b). Siderite precipitation is mostly associated with mica minerals in the Gassum Formation (Weibel et al., 2017a) so the rare siderite occurrence in Zealand is probably related to the smaller mica content, whereas siderite is occasionally very abundant in Jutland, especially in shoreface sandstones.

2.6.1. Mineralogy of the Hanstholm structure

The estimated maximum burial depths of c. 1600-1800 m in the Hanstholm structure corresponds to the maximum burial depths of the Gassum Formation in the Thisted-3 well, which is the closest cored offset well located c. 50 km south-southeast of Felicia-1. Hence, the mineralogical composition of the fluvial, estuarine, lagoonal and shoreface sandstone cores from Thisted-3 is expected to give a good indication of the mineralogy in the Hanstholm structure, while also considering the variation found in the remaining wells from Jutland, although not variations related to larger burial depth (Fig. 2.4). Some uncertainty is related to the interpretation of depositional environments in the Hanstholm structure but well-log patterns show that it is very likely that shoreface sandstones and perhaps also estuarine sandstones are present (Olivarius et al., 2019a) and seismic mapping of channels indicates that fluvial sandstones may also be present (Erik Skovbjerg Rasmussen, CCUS preliminary results). The provenance has been investigated in the Felicia-1 and J-1 wells and documents that the sediment is derived from the Fennoscandian Shield (Olivarius et al., 2019a) and is therefore part of the immature mineralogical province. The expected mineralogy in the Hanstholm structure is presented in Table 2.1.

2.6.2. Mineralogy of the Havnsø structure

The estimated maximum burial depths of c. 1900-2200 m in the Havnsø structure correspond fairly well to the amount of burial that the Gassum Formation in the Stenlille wells has been exposed to, which are the closest cored wells positioned c. 30 km southeast of the structure. The mineralogical composition of the sandstones in the Stenlille-15, -18 and -19 wells may therefore hint to the mineralogy present in the Havnsø structure (Fig. 2.4). However, large uncertainty is related to the interpretation of depositional environments in the Havnsø structure, which affect the interpreted mineralogical composition especially in relation to the amount of carbonate minerals. Large uncertainty is also associated with the provenance interpretation due to the critical position of Havnsø between a mature and an immature mineralogical province, where the expected mineralogy is based on the assumption that Havnsø has most resemblance to the eastern province, but if this is incorrect then the mineralogy will be more in line with what is expected for the Hanstholm structure. The expected mineralogy in the Havnsø structure is presented in Table 2.1.

Table 2.1. Expected mineralogy in the reservoir intervals of the Gassum Formation in the Hanstholm and Havnsø structures estimated from core data from other areas. The detrital clay occurs as matrix or clasts. The kaolinite, illite and chlorite contents refer to the authigenic clays. The amount of authigenic quartz is expected to be 0–3% in Hanstholm and 0–5% in Havnsø.

Hanstholm structure			
minerals	min (vol%)	average (vol%)	max (vol%)
Quartz	40	62	75
K-feldspar	2	8	15
Plagioclase	2	10	25
Mica minerals	0	1	12
Detrital clays	0	8	20
Rock fragments	0	2	6
Heavy minerals	0	1	3
Calcite/ankerite	0	2	40
Siderite	0	2	35
Kaolinite	0	2	6
Illite	0	0	10
Chlorite	0	0	5
Pyrite	0	1	25

Havnsø structure			
minerals	min (vol%)	average (vol%)	max (vol%)
Quartz	70	86	90
K-feldspar	0	3	9
Plagioclase	0	1	6
Mica minerals	0	0	2
Detrital clays	0	4	10
Rock fragments	0	1	3
Heavy minerals	0	0	1
Calcite/ankerite	0	1	40
Siderite	0	0	10
Kaolinite	0	2	6
Illite	0	0	5
Chlorite	0	0	1
Pyrite	0	0	5

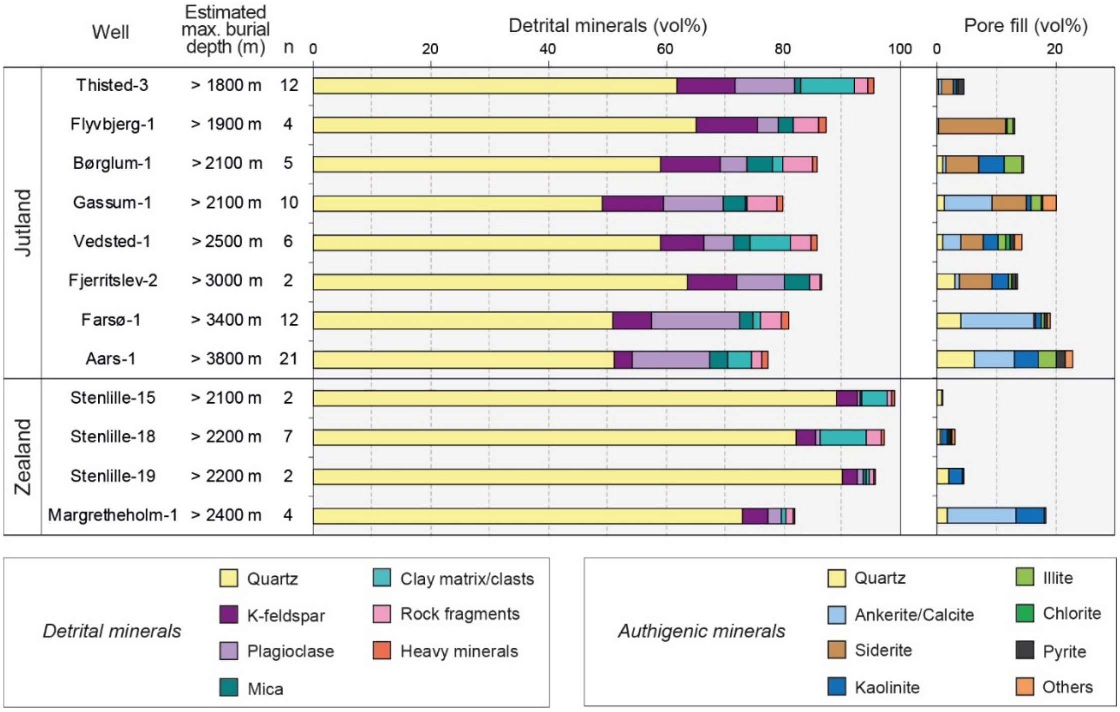

Figure 2.4. Mineralogical composition of the Gassum Formation based on point counting of thin sections (Vosgerau et al., 2016a; Weibel et al., 2017a). The depths represent the estimated maximum burial depths corrected for structural inversion (Japsen and Bidstrup, 1999; Japsen et al., 2007) and the mineralogical data are ordered with increasing depths for wells from the western (Jutland) and eastern (Zealand) regions, respectively. Increasing amounts of pore-filling minerals are found with increasing depth and the types of authigenic minerals change with depth. A larger mineralogical maturity is found in sandstones from Zealand as seen by e.g. the higher detrital quartz content. The analysed material is sampled from sandstone cores, except for the Margretheholm-1 well where only cuttings were available, so the high abundance of carbonate cement may be caused by the cemented cuttings being better preserved. The number of analysed samples is designated by 'n'.

2.7. Formation water chemistry

Although almost one hundred deep (> 500 m) wells have been drilled onshore Denmark, reliable formation water chemistry data were only obtained from relatively few of these wells. Until 1978, wells were mostly drilled for oil exploration purposes, and only few tests were performed since no commercial quantities of oil had been encountered. After 1978, drilling activities relating to geothermal energy, natural gas underground storage and nuclear high-level waste storage greatly enhanced our knowledge on formation water chemistry. An overview of existing knowledge of formation water chemistry of Danish saline formation waters is given in Laier (2008).

Figure 2.1 shows the location of existing deep wells from which formation water chemistry data for the Gassum Formation exist together with the location of the Havnsø and Hanstholm structures. No wells with pore water chemistry exist for either of the two structures and thus their pore water chemistry must be estimated from nearby wells. For the Hanstholm structure the closest well is the Thisted-2 well, while the wells closest to the Havnsø structures are the Stenlille-1 and Stenlille-19 wells. The pore water chemistry measured in the Gassum Formation in these wells is listed in Table 3.1.

While the pore water chemistry of the Thisted-2 well may give a reasonable estimate of the pore water chemistry in the Hanstholm structure, large uncertainties are related to the assumption that the pore water chemistry of the Stenlille wells may represent the pore water chemistry in the Havnsø structure. This uncertainty is mainly caused by the uncertainty related to the interpretation of depositional environments in the Havnsø structure as discussed above.

Table 3.1 Estimated formation water chemistry for the Havnsø and Hanstholm structures based on nearby wells (Laier, 2008).

Structure		Hanstholm	Havnsø	
Well		Thisted-2	Stenlille-1	Stenlille-19
Depth	m	1257	1510	1640
pH		6.4	6.2	
Cl	g/L	102	108	113
SO_4^{2-}	g/L	0.01	0.015	<0.02
Br	g/L	0.29	0.47	0.44
HCO_3^-	g/L	0.043	0.077	
Na	g/L	55	58	59
Ca	g/L	7.5	8.6	11.5
Mg	g/L	1.50	1.64	1.14
K	g/L	0.25	0.37	1.1
Sr	g/L	0.38	0.64	0.66
Fe	g/L	0.04	0.06	
NH_4	mg/L	52	60	
Ba	mg/L			39
Zn	mg/L	1		65
Li	mg/L	2		2.7
SiO_2	mg/L	26	16	

Injected CO_2 is soluble in the formation water with solubility strongly dependent on temperature, pressure and formation water salinity. Thus, CO_2 solubility decreases with increasing temperature and salinity and increases with increasing pressure (e.g., Takenouchi and Kennedy, 1964, 1965). Assuming a temperature of 30°C and a pressure of 97 bar at a depth of 900 m for the Hanstholm structure (pers. comm. Carsten Møller Nielsen), the solubility of CO_2 in the formation water at the Hanstholm structure is *c.* 680 mmol/L. The solubility of CO_2 in the formation water at Havnsø is *c.* 650 mmol/L, assuming a temperature of 43°C and a pressure of 158 bar at a depth of 1400 m.

3. The fate of CO_2 in the reservoir

In general, CO_2 injected into a saline reservoir may be trapped in the reservoir due to one of the following four processes (IPCC, 2005) (Figure 3.1):

1. *Structural and stratigraphic trapping*. The CO_2 trapped by this process represents CO_2 trapped in the pore space of the saline reservoir as a buoyant immiscible fluid phase. The process is controlled by large scale geological and lithological variations (m to km scale).
2. *Residual trapping*. The CO_2 trapped in small pores which cannot be mobilized anymore. The process is controlled by small scale geological heterogeneities (mm to cm scale).
3. *Solubility trapping.* The CO_2 trapped by this process represents CO_2 dissolved in the reservoir brine.
4. *Mineral trapping*. CO_2 incorporated into minerals due to chemical precipitation.

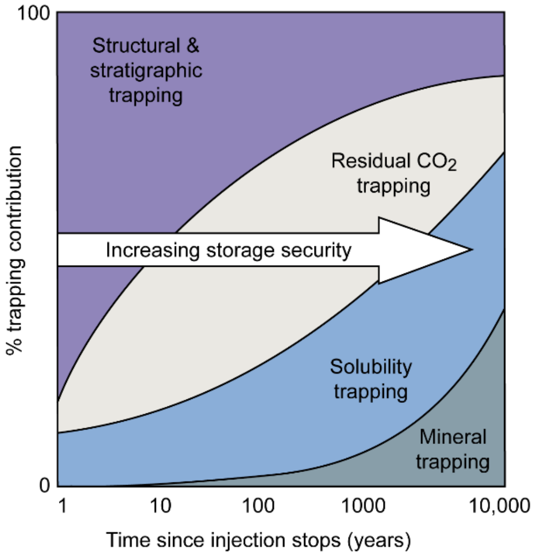

Based on IPCC, 2005

Figure 3.1: Four main trapping mechanisms are considered to be responsible for trapping of CO_2 in a saline aquifer. Storage security will most likely increase over time due to hydrogeochemical reactions in the reservoir (IPCC, 2005)

Regarding the impact for storage security, timescales for these four types of trapping mechanisms differ from one process to another (Figure 3.1). Chemical reactions in the reservoir are important mainly for the latter two trapping mechanisms and as such have the largest overall impact for storage security over longer time scales. However, solubility trapping is fast. In addition, at shorter time scales chemical reactions in the vicinity of the injection well may have an impact on the injection operation and as such determine the success of a CO_2 storage and utilization project. Thus, chemical reactions may e.g. result in corrosion (if proper material choices have not been made) and re-crystallization of well cement. Such chemical processes are outside the scope of the current report, but hydrogeochemical reactions such as fast dissolution of carbonate minerals and/or precipitation of salts due to desiccation may have an impact on the operation at shorter timescales as well. These processes are described in greater detail in section 4.

Pure and dry CO_2 is not reactive, but in aqueous solution a portion of the CO_2 will, depending on temperature and pressure, react with water (H_2O) to form carbonic acid (H_2CO_3) (eq. 3.1). Thus, CO_2 and H_2O readily dissolves in each other and causes solubility trapping (Figure 3.1). Carbonic acid in turn will dissociate into protons (H^+) and bicarbonate (HCO_3^-) (eq. 3.2). The bicarbonate ion again dissociates into a proton (H^+) and carbonate (CO_3^{2-}) (eq. 3.3). Altogether, the reaction between CO_2 and H_2O creates a low pH environment where the activity of the various carbonate species and the pH are determined mainly by CO_2 pressure, salinity and temperature. The set of chemical reactions determining the carbonate equilibria in a pure aqueous solution are (Appelo and Postma, 2005).

$$CO_2(g) + H_2O \text{ -> } H_2CO_3 \quad pK_H = 1.5 \qquad (3.1)$$

$$H_2CO_3 \text{ -> } H^+ + HCO_3^- \quad pK_1 = 6.3 \qquad (3.2)$$

$$HCO_3^- \text{ -> } H^+ + CO_3^{2-} \quad pK_2 = 10.3 \qquad (3.3)$$

Dissolution of CO_2 in the reservoir brine causes an increase of the brine density. If certain specific conditions prevail in the storage complex, this can eventually result in density driven transport of CO_2 enriched brine to deeper geological strata, which in such cases is expected to increase storage security even more over long time scales (e.g. Taheri et al., 2017).

On rearrangement of reactions 3.1-3.3, the reactions provide a general relation between the bicarbonate concentration in the brine, the CO_2 partial pressure, and the pH of the brine (Appelo and Postma, 2005):

$$\text{Log } [HCO_3^-] - \text{pH} - 7.8 = \log [P_{CO2}]$$

Thus, in a saline reservoir where the partial pressure of CO_2 increases due to CO_2 injection, pH will decrease, and the bicarbonate concentration will increase. It is the decrease in pH that causes the dissolution of rock forming minerals, which over longer time scales is a prerequisite for subsequent mineral trapping of the CO_2 through precipitation of other minerals. The amount of CO_2 that will eventually be trapped by mineral trapping is highly dependent on the specific mineral composition of the target geological formation for a specific CO_2 storage project.

Although chemical reactions over longer time scales are considered to increase the safety of a storage complex, they may also have other impacts during the lifetime of a CO_2 storage project. For example, mineral dissolution is expected to increase porosity and permeability and as such increase both storage capacity and injectivity (e.g. Gaus et al., 2008; Aminu, et al., 2017). However, mineral dissolution may also be critical to the mechanical strength of the reservoir if rock cementing minerals are dissolved because of the CO_2-rock interactions (e.g. Torsæter and Cerasi, 2018). On the longer term and if desiccation occurs, mineral precipitation may result in decreased porosity and permeability, and depending on where the minerals precipitate, such chemical processes may be the reason for challenges of a specific storage project (e.g. Gaus et al., 2008; Aminu et al., 2017; Torsæter and Cerasi, 2018).

4. Geochemical induced problems/possibilities

4.1. Dissolution and precipitation of minerals in storage formation

Years of research have demonstrated that substantial mineral dissolution and precipitation can occur upon interaction between rock, water and CO_2 at the conditions expected for storage. The results of experimental and numerical studies form the backbone of several reviews (Jun et al., 2013; Hellevang et al., 2013; Kampmann et al., 2014) and many newer studies exist (e.g., Davila et al., 2020; Fuchs et al., 2019). In our description of mineral dissolution and precipitation, we will first provide a brief background on mineral reactivity and then move on to describe the role of the two processes during CO_2 storage in saline aquifers in felsic, siliciclastic sediments with a focus on the Gassum formation.

The rock of the storage formation has for millions of years interacted with the surrounding water. This means that many minerals are in equilibrium with the solution and the remaining minerals are reacting very sluggishly because of kinetic hinderances. The degree of equilibration for a given mineral is commonly expressed as the saturation ratio, Ω, between the ion activity product (IAP) and the solubility product (Ksp) of the mineral. For calcite, for example, which dissolves through the reaction $CaCO_3 + H^+ = Ca^{2+} + HCO_3^-$, Ω is given by:

$$\Omega = \frac{IAP}{Ksp} \tag{4.1}$$

where:

$$IAP = \frac{(Ca^{2+})_{ac}(HCO3^-)_{ac}}{(H^+)_{ac}} \tag{4.2}$$

and:

$$Ksp = \frac{(Ca^{2+})_{eq}(HCO3^-)_{eq}}{(H^+)_{eq}} \tag{4.3}$$

In the equations, *$(X)_{ac}$* represent the actual activities of ion X in solution and *$(X)_{eq}$*, the activities expected at equilibrium. When a mineral is in equilibrium with the surrounding water, Ω equals 1 and no net dissolution or precipitation occurs. At undersaturated conditions, $1 > \Omega \geq 0$, minerals will dissolve, and at supersaturated conditions, $\Omega \geq 1$, they can precipitate.

The dissolution of CO_2 and the accompanying decrease in pH shifts the original equilibrium so that many minerals become undersaturated. For the calcite reaction equation, (H^+) increase disproportionally compared to the activity of the other reaction products. This means that the value for IAP will shift substantially below 1, so that dissolution is thermodynamically favoured until the mass transfer from the calcite re-establishes equilibrium. This thermodynamic destabilisation of minerals by decreased pH affect all metal oxides, carbonates, sulphides and multioxide silicates (i.e., $A_xSi_yO_z$, where A represents cations different from Si and x, y and z, stoichiometric coefficients). Thus, CO_2 injection yields a thermodynamic drive for dissolution of many minerals.

The rate for mineral dissolution varies widely. Evaporite minerals react fast, for example, whereas silicate minerals typically dissolve much slower. For many minerals, the bonding between the atoms become weakened when H^+ becomes affiliated with the surface. Hence, dissolution rates are often pH dependent. In addition, dissolution slows as the solution becomes increasingly saturated (i.e., when Ω approaches 1).

Much is known about the dissolution rate for specific minerals. Traditionally, equations for the rate of mineral dissolution and their dependence on pH (or other ions) are expressed as:

$$r_+ = A_a\, e^{\frac{-E_{a(a)}}{R}\frac{1}{T}}(H^+)^n + A_n\, e^{\frac{-E_{a(n)}}{R}\frac{1}{T}} \qquad (4.4)$$

Here, r_+ is the surface normalised dissolution rate at far from equilibrium for a given mineral (mol/m^2/s); A_a and A_n are preexponential factors for the reactions at acidic and the neutral conditions (mol/m^2/s), $E_{a(a)}$ and $E_{a(n)}$, the corresponding activation energies of the reactions (kJ/mol); R is the gas constant (8.314 $*10^{-3}$ kJ/mol/K); T, the absolute temperature (K); (H^+), the activity of the proton; and n is the reaction order with respect to proton activity.

As dissolution reactions progress, the solution becomes increasingly saturated with respect to the dissolving minerals, which slows dissolution rates. To account for this, the net dissolution rate per surface area (r_{net}) is often calculated by:

$$r_{net} = r_+\,(1 - \Omega) \qquad (4.5)$$

or similar expressions.

Several compilations have been made of far from equilibrium dissolution rates determined in the laboratory (e.g., Palandri and Kharaka (2004) and Brantley (2008), which contain data for many minerals, and Rimstidt et al. (2012), which critically compiles dissolution rates for a single mineral, in this case forsterite). Figure 4.1 shows dissolution rates at far from equilibrium for a range of silicates and for calcite and siderite at 80°C calculated from data given in Palandri and Kharaka (2004). Clearly, the dissolution rates vary hugely. Some minerals, for example calcite, dissolves very quickly, whereas others, e.g., muscovite, dissolves much slower (up to 10 orders of magnitude). Most minerals show higher dissolution rates at lower pH. Thus, the acidification caused by CO_2 dissolution not only shifts the solution away from equilibrium with respect to the minerals, it also increases the mineral reaction rates.

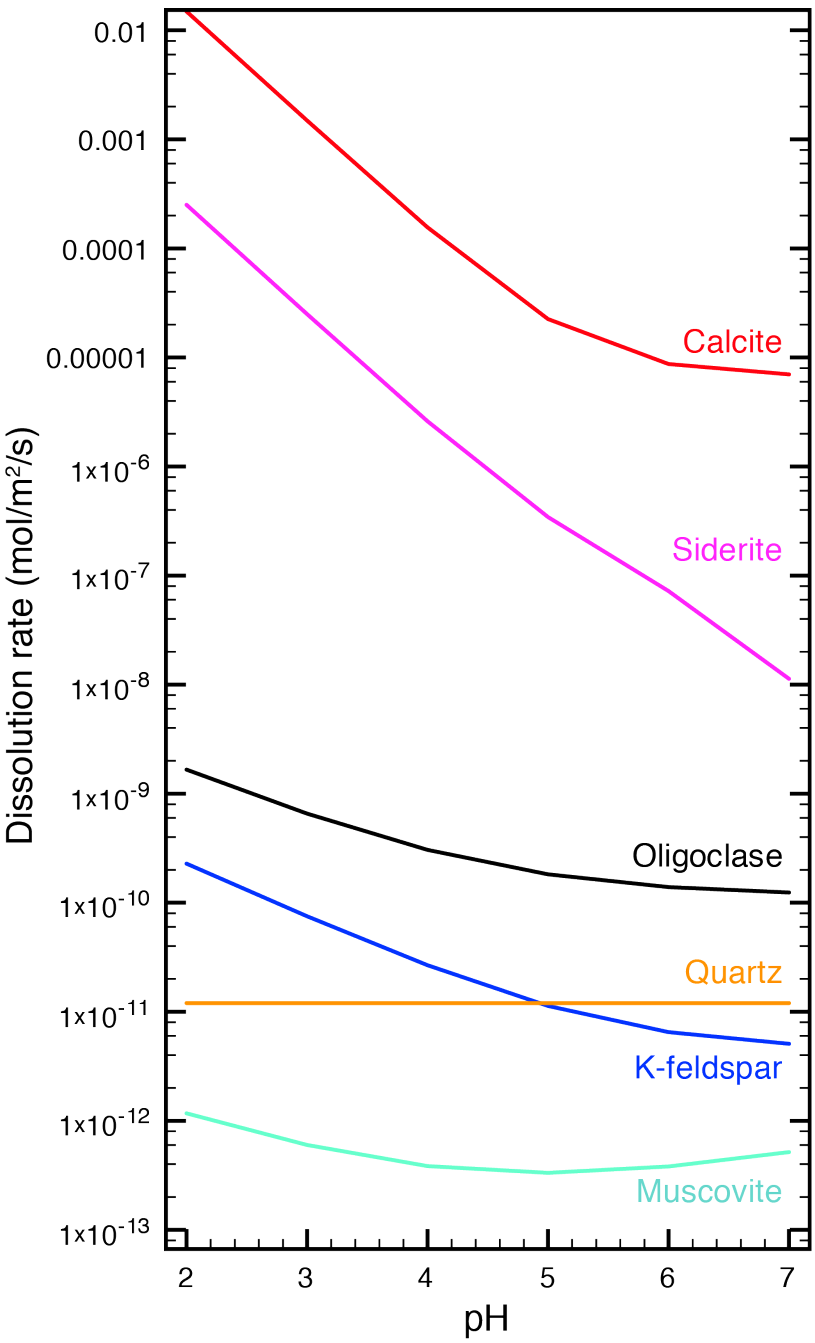

Figure 4.1 Far from equilibrium dissolution rates (logarithmic scale) of example silicates and carbonates as a function of pH. Calculated using data from Palandri and Kharaka (2004).

Even though quantification of mineral dissolution rates has been one of the focus areas in geochemical research for decades, mineral dissolution is complex, in particular for multioxide silicates. Determined dissolution rates often show significant discrepancies between different laboratories (± 2 orders of magnitude; Brantley, 2008) and even for studies conducted by the same laboratory (± a factor of 4). The nature of the mechanisms responsible for the observed dissolution rates are disputed (e.g., Oelkers, 2001; Dove et al., 2005; Hellmann et al., 2015), and dissolution rates estimated at field scale often deviate by an order of magnitude or more from those determined in the laboratory for reasons that are not fully understood (e.g., Brantley, 2008); reasons could include slowing of reaction rates from surface precipitates of secondary minerals, the formation of Si rich, leached layers, or erroneous correction of decreased reaction rates as solutions approach saturation with respect to the dissolving mineral (e.g., Kampmann et al., 2014). In addition, the solubility of some minerals is poorly described, in particular at the elevated salt concentration, temperature and pressure of CO_2 storage (e.g., Kampmann et al., 2014). Thus, the results of calculations based on mineral dissolution rates must be interpreted with caution.

4.2. Dissolution and precipitation reactions with impact on storage

4.2.1. Near-well reactions in the formation during injection of pure CO_2

As supercritical CO_2 is injected into the reservoir, it is expected to displace most of the water and migrate upward because of its lower density. Some residual water will be trapped in pore spaces because of surface tension, generating a zone with two phase saturation. Assuming that the supercritical CO_2 is unsaturated with respect to water (dry CO_2), dissolution of water in the CO_2 will remove the residual water closest to the well. These processes will most likely create three zones around the injection point and the upward migrating CO_2 (see Fig. 4.2 for sketch):

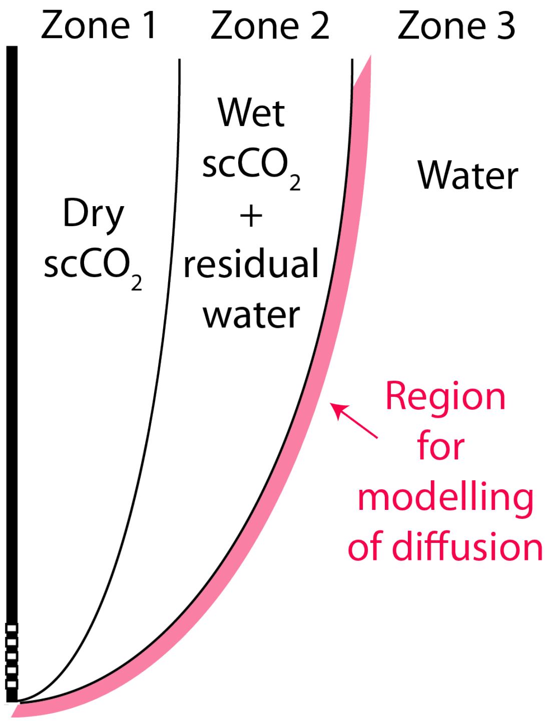

Figure 4.2 Sketch of the phase saturation of the near-well during injection with indication the location of the system modelled with diffusion (light red).

Zone 1: Close to the well, all water will be removed by the injected CO_2 because of drying.
Zone 2: A region containing both water saturated CO_2 (wet CO_2) and residual water.
Zone 3: More distant, pore spaces will be completely filled with water, which would become gradually acidified by dissolved CO_2 with time.

The spatial distribution of the zones will depend on many parameters, such as the manner by which the injection is conducted (CO_2 and water injection may be alternated for example), the flow rates and paths for both phases, and their variation with time because of fluctuating injection rates and changes to the permeability caused by geochemical reactions. This produces a system so complex that computational modelling capable of coupling flow and reactivity is required to understand its behaviour. Thus, we shall limit our investigations to selected, more tractable aspects.

During the injection of the CO_2, it is imperative that injectability remains intact. In Zone 1, mineral dissolution and precipitation is likely to be minor, because water is absent or occur in low concentration in the CO_2. A number of studies have suggested that desiccation in Zone 1 could cause salt precipitation which may eventually have a negative impact on porosity and permeability in the zone near the injector well – and thereby on injectivity in the reservoir (Azaroual et al., 2007; André et al., 2007; Pruess and Müller, 2009; Peysson et al., 2011). These studies are all based on numerical simulations alone and evaluates the effect on the total porosity and absolute permeability relative to a dry sandstone without salt precipitated. Other studies (e.g. Ott et al., 2011) with an experimental approach suggest that although salt precipitation occurs due to desiccation, and a substantial impairment of the absolute permeability can be observed, the effective CO_2 permeability increases due to the removal of brine by desiccation. Thus, overall the desiccation is not expected to have a major impact in highly porous and permeable sandstones such as the Gassum Formation sandstones.

In Zones 2 and 3 around the well, CO_2 charged waters will result in mineral dissolution. This could cause removal of the cement that binds the grains together, decreasing rock strength and lowering the pressure at which fracturing occurs (e.g., Rackley, 2017). Alternatively, the dissolution of one mineral could provide the building blocks for precipitation of another mineral. If such secondary minerals grow in pore throats, permeability will decrease.

Given that the injection period would be relatively short, 10–20 years, dissolution of the most sluggish reacting silicates would most likely not be of great importance. The Gassum formation does, however, contain appreciable amounts of calcite and siderite, which would dissolve quickly until the waters reach equilibrium with respect to the carbonates. At 80 °C and 100 atm CO_2 partial pressure, the solubility of calcite in 1 M NaCl water is roughly 30 mM and of siderite, 0.4 mM. Compared to the amount of calcite and siderite present in the formation, this is negligible. Even though diffusion would transport the dissolved components of the carbonates from the site of dissolution, this process would most likely be so slow that it would not critically increase the amounts of carbonates that dissolve. These considerations suggest that carbonate dissolution would be minimal in the absence of water flow, and unlikely to cause substantial loss of the formation's geomechanical strength.

In several parts of this report, we will conduct calculations to evaluate if mineral dissolution and precipitation affect the nature of the rock using 1D reactive transport modelling with the geochemical software PHREEQC (Parkhurst and Appelo, 2013) and its native database. The details of the methods are presented in Appendix 1. Briefly, the rock composition was approximated based on results Table 2.1, using an average composition for the two sites, and the brine composition was calculated to yield equilibrium with respect to the minerals in the formation that were not thermodynamically highly unstable, and hence likely to be kinetically hindered in dissolution. Compared to the brine analyses, the calculated brine is less concentrated in Na and Cl, which would mean that CO_2 dissolution would be somewhat overestimated.

The first set of calculations surveys the geochemical reactions occurring in the water of the near-well environment in the absence of water flow (i.e., considering only transport by diffusion). The calculations were intended to simulate the transport of aqueous species and the mineral reactions occurring in the 2 m of formation water closest to a stagnant interface between wet $scCO_2$ in Zone 2 and the completely water saturated Zone 3 (location of system highlighted in light red in Figure 4.2). The calculations were carried out for 20 years and they were based on 200 cells of 2 cm. In the calculations, the first cell contained an infinite amount of CO_2 with a pressure of 100 atmosphere that could dissolve in the water of cell 1. Transport of aqueous species between the cells occurred solely through diffusion with an effective diffusion coefficient set to 10^{-9} m^2/s for all species, reflecting a porosity of 20% and increased diffusion rates at elevated temperature (e.g., a factor ~3 higher for CO_2 compared to room temperature; Zeebe, 2011).

The results of the calculations are given in the left column of Figure 4.3. During the 20 years simulated, a low pH front propagates from the CO_2/water interface into the sediment reaching a distance of ~2 m. The acidification of the water causes some dissolution of calcite, but this is limited to the first cell of the sediment and the amount of dissolved calcite constitute only 6% of the available calcite in the cell. Although transport through diffusion does cause increased calcite dissolution compared to our simpler calculations above, the extend of dissolution most likely will not affect the rock strength. The calculations indicate that siderite dissolution will be negligible, reflecting this mineral's lower solubility.

As the low pH front propagates into the sediment, it causes silicate dissolution through reactions of the kind:

$$\underset{\text{(oligoclase)}}{Na_{0.8}Ca_{0.2}Al_{1.2}Si_{2.8}O_8} + 8\ H_2O = 0.8\ Na^+ + 0.2\ Ca^{2+} + 1.2\ Al(OH)_4^- + 2.8\ H_4SiO_4, \qquad (4.6)$$

This increases the dissolved concentrations of Na, Ca, Al and Si, and causes saturation of the solution with respect to calcite, amorphous silica and kaolinite. Upon saturation, these minerals precipitate in the model and the net reaction for oligoclase becomes that of mineral replacement:

$$\begin{aligned} &Na_{0.8}Ca_{0.2}Al_{1.2}Si_{2.8}O_8 + 0.8\ H_2O + 0.2\ CO_{2(aq)} + 0.8\ H^+ \\ &\qquad = 0.8\ Na^+ + 0.2\ CaCO_3 + 1.6\ SiO_{2(am)} + 0.6\ Al_2Si_2O_5(OH)_4 \qquad (4.7) \end{aligned}$$

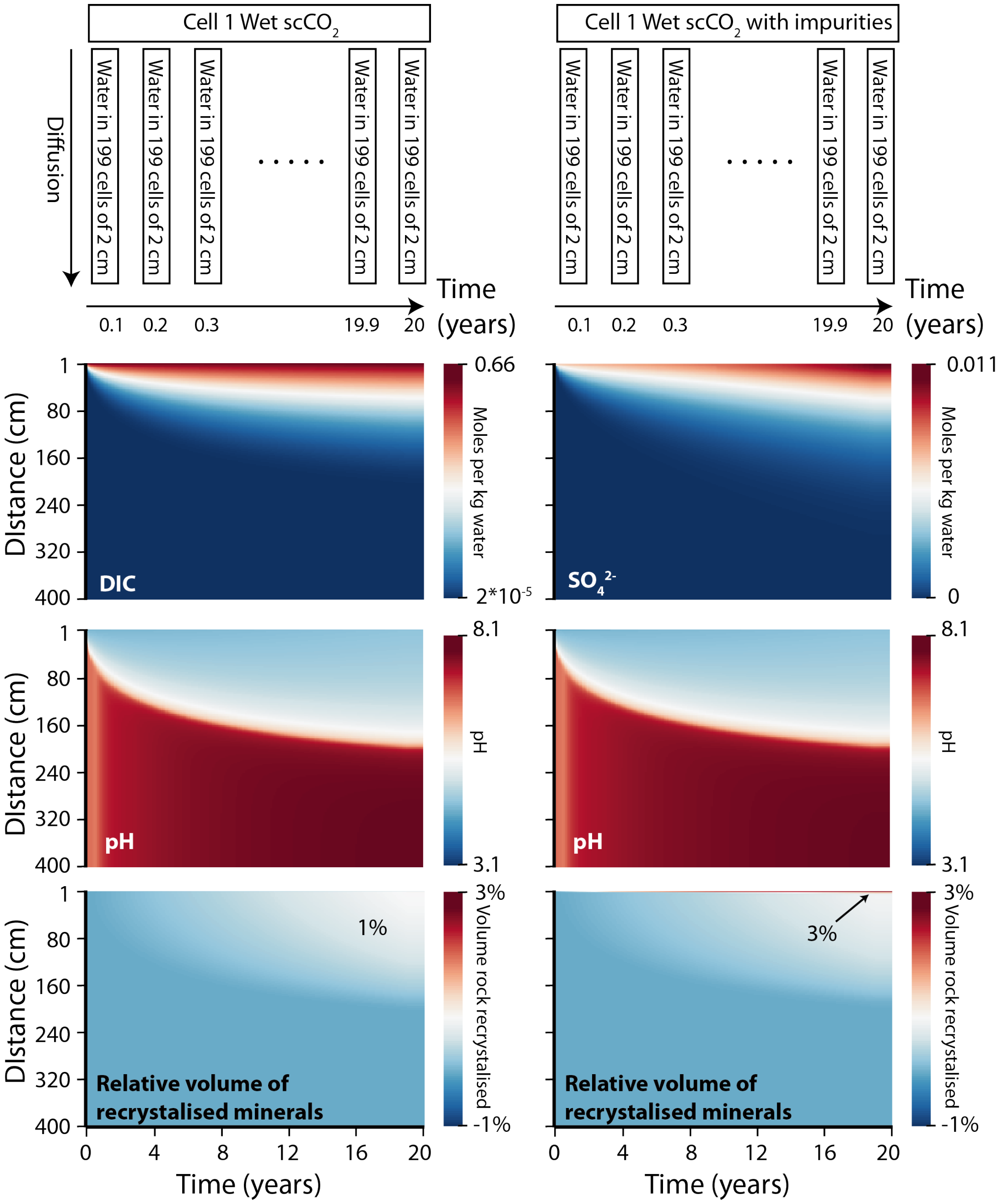

Figure 4.3 Schematic representation of PHREEQC model and example results for the calculations of 1D reactive transport modelling with diffusion. The left column shows results of calculations with pure CO_2, whereas the right column gives those for CO_2 with 1000 ppm O_2 and 100 ppm SO_2.

Thus, the calculations predict that calcite, amorphous silica and kaolinite will form in the first 2 m (excluding the sediment in the cell closest to the interface), causing a decrease in the total amount of dissolved CO_2 (dissolved inorganic carbon; DIC). The amount of new formed material is small, though, accounting for a maximum of 1% of the rock volume or 4% of the pore volume. This amount is most likely an overestimation, given that we have used silicate dissolution rates in the higher end of those probable. To conclude, the calculations indicate that alterations to the rock will be fairly small if diffusion is the only transport process that operates. Thus, the risk of adverse changes to the rock properties because of geochemical reaction is low as long as water flow is negligible. This does, however, not exclude that injection is hampered by other processes, such as clogging caused by transport of colloids present naturally in the formation or introduced through the gas stream.

4.2.2. Near-well reactions in the formation during injection of impure CO_2

The injected CO_2 is likely to contain some impurities, such as H_2, N_2, Ar, O_2, H_2S, CH_4, SO_x and NO_x. Some of these gases are quite reactive, notably O_2, SO_2 and NO_2 which give rise to acidification (e.g., Knauss et al., 2005; Pearce et al., 2019; Spycher et al., 2019). This additional acidification is localised primarily around the injection well because the gases react rapidly (Spycher et al., 2019). The induced acidity can cause dissolution of carbonate minerals and for SO_2, formation of sulphate and sulphide minerals (e.g., Hedayati et al., 2018). Upon dissolution, SO_2 and NO_2 disproportionates via the reactions:

$$SO_{2(aq)} + H_2O = 1.75\ H^+ + 0.25\ HS^- + 0.75\ SO_4^{2-} \qquad (4.8)$$

$$2\ NO_{2(aq)} + H_2O = 2\ H^+ + NO_2^- + NO_3^- \qquad (4.9)$$

and the HS^- produced via the reaction in EQ. 4.8 can react further with oxygen:

$$O_{2(aq)} + 0.5\ HS^- = 0.5\ H^+ + 0.5\ SO_4^{2-} \qquad (4.10)$$

All of these reactions produce acid. In addition, they produce SO_4^{2-}, which can combine with dissolved Ca^{2+} to form anhydrite or gypsum, and HS^- (at least as an intermediate species), which can combine with Fe^{2+} to produce iron sulphide. Finally, O_2 may react with Fe^{2+} to produce Fe(III) oxides. The presence of these redox active impurities clearly amplifies the number of reactions that are possible, greatly complicating predictions of the temporal evolution of the rock composition.

To evaluate to what extent mineral reactions are likely to increase in the presence of impurities, the 1D transport modelling with diffusion was repeated with a simplified CO_2 phase containing 1000 ppm O_2 and 100 ppm SO_2. These concentrations are in the high end of those expected for impure CO_2 (Rackley et al., 2017). In the calculations, rates for the reactions in EQ. 4.8 and EQ. 4.10 were taken from Spycher et al., 2019:

$$r = 2.6*10^{-6} * [SO_{2(aq)}] \qquad (4.11)$$

and

$$r = 8.54*10^{-5} * [O_{2(aq)}]^{0.2} * [HS^-]^{0.82} \qquad (4.12)$$

Although the value for the rate constants are valid for 65°C and not the 80°C otherwise assumed, this discrepancy was considered minor compared to those arising from other sources. To simplify the calculations, the oxidation of Fe^{2+} by O_2 was ignored and all redox active species were allowed to be out of redox equilibrium. Compared to the diffusion calculations with pure CO_2, two additional phases were allowed to form when supersaturated: anhydrite and mackinawite, which is a poorly crystalline, metastable FeS that typically forms as a precursor for more stable iron sulphides.

The results of the calculations with impurities are largely similar to those of the diffusion calculations with pure CO_2, with substantial differences only occurring in the first two cells (4 cm; right column in Figure 4.3). Here, significant dissolution occurs for calcite (~40%) and for siderite (~10%) with concomitant precipitation of anhydrite and mackinawite:

$$CaCO_3 + SO_4^{2-} + H^+ = CaSO_4 + HCO_3^- \tag{4.13}$$

and

$$FeCO_3 + HS^- = FeS + HCO_3^-. \tag{4.14}$$

These reactions mean that the volume of new formed minerals amounted to ~3% of the rock volume (or 12% of the porosity). This is three times that predicted for the pure CO_2 system. Given that the reactions affect primarily the sediment closest to the supercritical phase, similar reactions are expected to occur in the mixed saturated Zone 2, to the extent that water is in contact with carbonate.

The estimation of the amount of material formed is independent of the rate of silicate dissolution chosen for the calculations, which could have yielded unrealistically fast mineral formation rates. Instead, it relies on diffusion and the reaction rates for the gases. These are reported for a homogeneous system (i.e., without solid surfaces). Similar to other redox reactions (e.g., Fe(II) oxidation by O_2; Tamura et al., 1976), heterogeneous reactions on the surfaces of solids may be much faster. Thus, the rate of redox reaction for the gases may well be faster in reality.

Clearly, the calculations do not allow us to pinpoint the location of the new formed material, but the amount of material is such that it could substantially affect permeability if solids preferentially nucleate and grow in pore throats. Given that i) reaction rates may be faster than modelled, ii) the calculations only survey one of many possible reaction pathways, and iii) flow of water may occur for some of the injection scenarios, which could increase the degree of alteration, we find that the presence of impurities substantially elevates the risk for adverse changes to the rock properties in the near-well environment. We recommend that the system be studied further through more detailed modelling and, possibly, laboratory experiments.

4.2.3. *Mineral reactions affecting density driven flow, solubility trapping and mineral trapping*

When the plume of supercritical CO_2 has settled at the top of the storage formation, CO_2 will dissolve into the water at rates that are initially controlled by diffusion. The first 20 years of this process is probably captured reasonably well by the simulations presented in Figure 4.3. The dissolution of CO_2 slightly increases the density of the formation water, and once a critical thickness of CO_2 charged water has been reached, density driven, convective flow (fingering) will commence (e.g., Preuss and Zhang, 2008; Pau et al, 2010; Sketch in Fig. 4.4A).

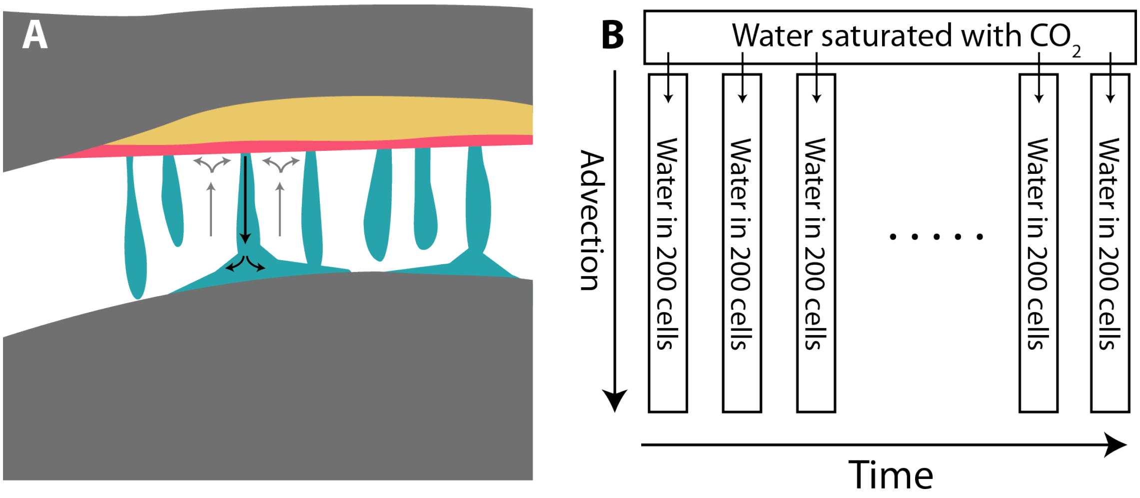

Figure 4.4 A) Sketch of the density driven convection of CO_2 charged water (modified from Lykke Sandals figure in Geoviden, 2020). The region with initial transport controlled by diffusion is light red. Flow from density driven convection indicated by arrows and the resulting CO_2 fingers given in green. B) A schematic representation of PHREEQC model representative for the processes occurring along the black arrows in A.

To estimate possible changes to the rock because of geochemical reactions during slow, density driven flow, we performed a set of 1D reactive transport calculations with flow of CO_2 charged water through the sediment (general details of methods in Appendix 1). The calculations were based on 400 cells with influx of formation water saturated with respect to 100 atm CO_2 into cell 1 to reflect dissolution of CO_2 in formation water flowing past the supercritical CO_2 during the density driven convection. Finally, transport through cells occurred by advection and the effect of dispersion were ignored.

The actual velocity of the density driven flow depends on the density and viscosity of the water and the vertical permeability of the formation (Pau et al., 2010). Assuming that the vertical permeability is identical to the average measured gas permeability for the Gassum formation, which is about 0.1 mD (or ~$10^{-13}$$m^2$) for a porosity of 20% (Weibel et al., 2020), the velocity of the flow through the sediment will be approximately 1 m per year (Preuss and Zhang, 2008). However, measured gas permeability varies substantially (Weibel et al., 2020) and vertical permeability may be lower than the measured gas permeability. Thus, the flow velocity is poorly constrained. To determine the effect of different flow velocities, two set of calculations were performed; one set of calculations where solutions resided for 0.1 year in each cell and another set with a residence time of 1 year. The calculations were performed to have the CO_2 charged water reach cell 400, i.e., for 40 years or for 400 years. This could represent flow with a velocity of 10 or 1 m per year through 400 m of sediment. This thickness is somewhat too high for the Gassum formation, meaning that some of the cells represent flow along a sloping sediment in the bottom of the formation. The change in velocity for such flow has been ignored. A schematic rendering of the model is given in Figure 4.4B.

Examples of the results of the calculations are shown in Figure 4.5 for the amount of oligoclase, calcite and kaolinite in the cells as a function of time. The solution flowing into the cells have a pH of about 3.1 after equilibration with the free phase CO_2 at 100 atm located at the top of the formation (i.e., outside the cells). In cell 1 and 2, the constant propagation of this acidic solution causes dissolution of calcite (magnified insert above the calcite plots):

$$CaCO_3 + H^+ = Ca^{2+} + HCO_3^- \qquad (4.15)$$

For both sets of calculations, however, calcite dissolution is confined to cell 1 and 2, reflecting the relatively low solubility of calcite, even at elevated CO_2 partial pressure. Thus, the reactive front causing extensive calcite dissolution progresses very slowly.

In contrast, the amount of dissolved oligoclase depends both on the solubility as well as the reaction rates. After reaction with calcite in cell 1 and (later) cell 2, the water remains acidic and it is highly undersaturated with respect to oligoclase. Consequently, dissolution of the mineral progresses relatively rapid. This causes pH to increase from ~4.5 to ~7 and precipitation of calcite, $SiO_{2(am)}$ and kaolinite through the reaction given in EQ. 4.7. Thus, if the density driven flow is slow, as simulated in the 400 years calculations, oligoclase could become completely dissolved in the upper part of the sediment column, causing substantial formation of calcite. The reactive front responsible for this alteration propagates slower downwards than the actual CO_2 charged waters, but much faster than the reaction front leading to dissolution of calcite.

Caution should be applied when interpreting these results. Long term dissolution rates, for example, are likely to be slower than those used in the calculations and the temperature used is in the upper range for CO_2 sequestration. In contrast, the vertical permeability may be lower than given by the gas permeability, meaning that the residence time could be substantially longer in the cells. These changes would have opposite effect on the location of the reactions, and they might largely cancel out in terms of spatial distribution (but not temporal distribution). Thus, compared to the calculations with a residence time of 1 year, simulations conducted with 1/10 of the dissolution rate for the silicates and a residence time of 10 years per cell (reflecting vertical permeability of 0.01 mD) yield the same pattern as the right hand column of Figure 4.5, except that the time is multiplied by 10 to give 4000 years.

Our calculations indicate that it is entirely possible that density driven flow may result in substantial silicate carbonation if the flow velocity is slow. This could decrease the porosity from the initial 20% to 19% in the cells, where the oligoclase transformation front has passed (Fig. 4.5). In contrast, carbonate dissolution can increase porosity to about 25%, but this change is confined to the region just below the free phase CO_2. The impact of such changes in porosity on flow requires coupling of geochemical reactions with flow modelling, which is

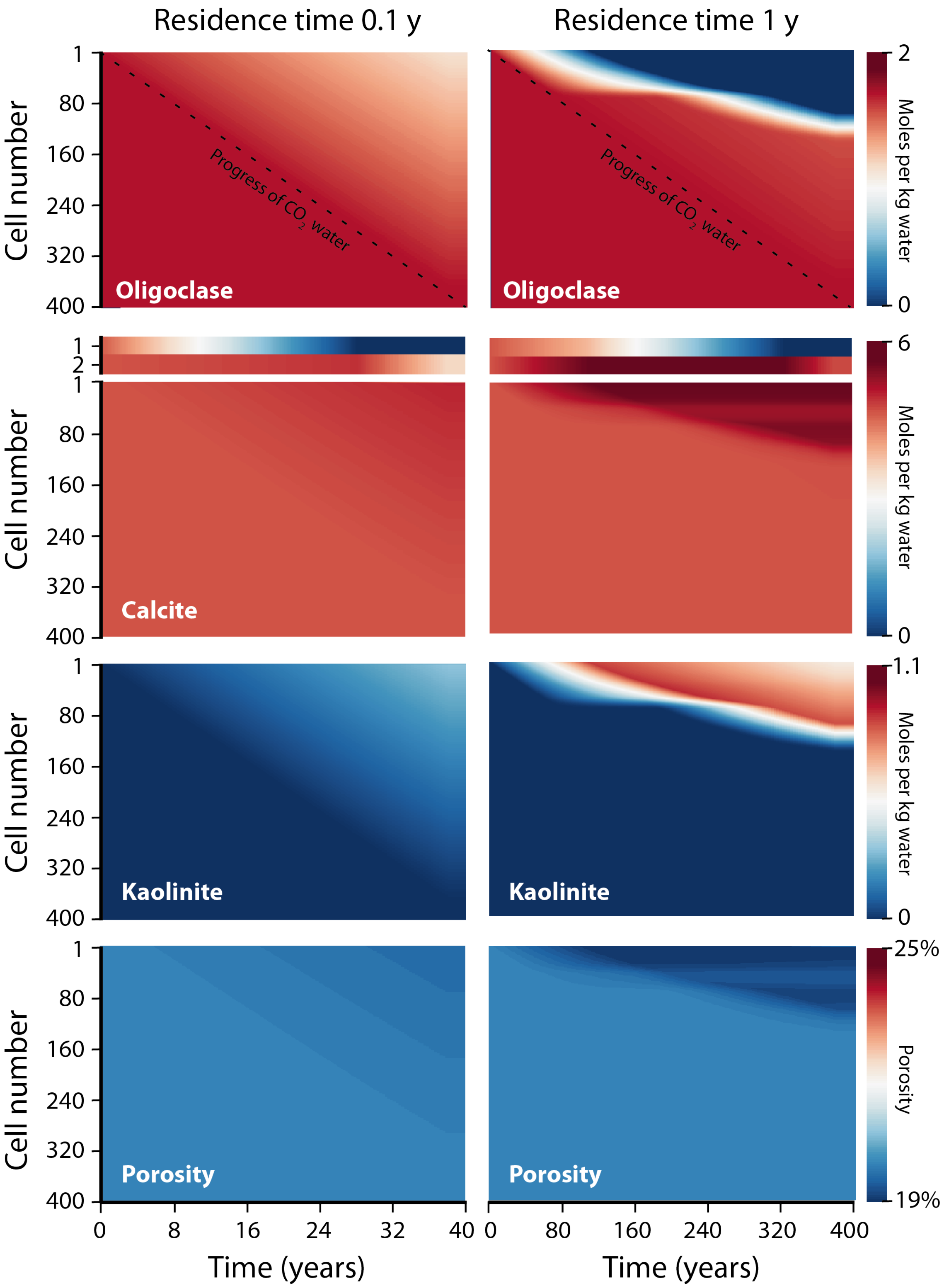

Figure 4.5 Example results for the calculations of 1D reactive transport modelling with advection. The left column shows results of calculations with a residence time of 0.1 year in each cell, whereas the right column shows results for a residence time of 1 year in each cell.

beyond the scope of this report. However, published modelling results suggests that the mineral carbonation could impact flow (Erfani et al., 2020). If the slight decrease in porosity from mineral carbonation changes permeability enough to make density driven flow more favourable elsewhere, the results may be that the "fingers" can only propagate for a certain period until reaction diverts the flow to a different location. This could increase the degree of interaction between rock and CO_2 charged waters, promoting mineral carbonation, but the disrupted flow might also slow the dissolution of CO_2 (and solubility trapping). Given the importance of solubility and mineral trapping on the long term safety of the storage facility, we recommend that modelling be conducted to understand the coupling of flow and geochemical reactions.

The calculations allow a very rough estimate of the time scales at which solubility trapping and mineral trapping can take place. Taking the calculations with a vertical permeability of 0.01 mD and a slowed silicate dissolution rate (by 1/10) as the most probable scenario, the results allow us to calculate the amount of CO_2 dissolved and that trapped in new formed calcite in all cells as a function of time. Given a cell length of 1 m and a cell volume of 1 L (1 dm^3), the area of the horizontal surface of the cells must be 0.1 dm^2. Using this horizontal area for the amount of CO_2 trapped in the cells, we calculate that after 4000 years ~6 ton of CO_2 could be solubility trapped per m^2 with density driven fingering, whereas 4 ton could be mineral trapped (Fig. 4.6). In the calculations, a temperature of 80 °C was used and a too dilute brine composition. Redoing the calculations at 50 °C and a more realistic brine composition (with 3 M NaCl) results in a solubility trapping of ~7 ton of CO_2 per m^2 and a mineral trapping of ~3 ton, i.e., values that are not substantially changed. For these calculations, however, the salinity is so high that the PHREEQC thermodynamic database is likely to yield somewhat incorrect results. Thus, for a CO_2 plume covering 1 km^2 with fingering occurring in 10% of the area, the calculated amount of CO_2 trapped after 4000 years of density driven convection amounts to approximately 0.6 Mton as solubility trapping and 0.4 Mton as mineral trapping.

Clearly, the calculations involve numerous simplifications and assumptions as well as parameters that are highly uncertain. Consequently, they should be viewed as preliminary efforts indented to provide a basic impression of the time scales at which trapping may occur, when mineral reaction rates are taken into account. Given the importance of the evolution of CO_2 trapping mechanisms with time, additional work is needed. Because of the time scales at which the trapping mechanisms evolve, this can best be accomplished with computational reactive transport modelling.

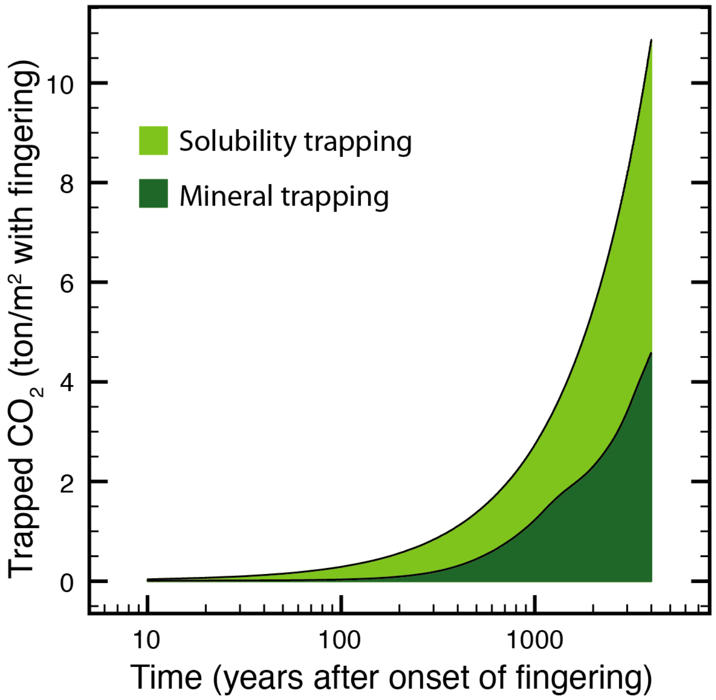

Figure 4.6 Calculated amount of CO_2 in solubility and mineral trapping as a function of time.

4.3. Particle mobilisation

Recent studies show that physical pore obstruction by fines migration may pose an injectivity issue during CO_2 injection into sandstones (Sbai and Azaroual, 2011; Sokama-Neuyam and Ursin, 2015; Al-Yaseri et al., 2017, Sokama-Neuyam et al., 2017; Xie et al., 2017; Othman et al., 2018). The observation of fines in the effluent together with an increase in the porosity due to dissolution of minerals led the authors to conclude that fines migration is responsible for the observed permeability decrease in core flooding experiments. Fines migration is a well-known mechanism of permeability reduction in otherwise high permeability sandstones in the context of geothermal as well as oil and gas production (e.g., Civan, 2007).

Fines are typically defined as mobile particles of an equivalent diameter smaller than 40 µm. The fines may be introduced to the sandstone formation by the injected fluid (Sharma et al., 2000), from contamination of the fluid by contact with drilling mud or filter cake residue on the wellbore wall (Venkitaraman et al., 1995), or be resident in the formation itself. In sandstone formations, fines are mostly mobilised clay particles present on the surface of matrix grains. Geochemical CO_2-brine-rock reactions could also generate secondary minerals into the pore fluid (Wilkinson et al., 2009; Ilgen and Cygan, 2016). Bicarbonate formed by dissolution of CO_2 in the formation water could react with cations in the rock and formation water to form stable carbonates e.g. $CaCO_3$, $MgCO_3$ or $FeCO_3$. These carbonates in solution could form other secondary minerals, aggregate into tiny particles in the bulk liquid or form a scale on the pore walls (Sayegh et al., 1990).

The mobilisation of fine particles in the reservoir is typically explained by applying force balance. Thus, when the sum of repulsive forces acting on a particle exceeds the sum of attractive forces, the particle is mobilised. The pH and salinity of the formation water, flow rate and temperature has been identified as some of the underlying parameters for particle mobilisation (Muecke, 1979; Khilar and Fogler, 1998). A critical salt concentration exists below which the pore fluid could weaken the Van der Waal's forces holding fine particles to the pore wall (Khilar and Fogler, 1983). Additionally, a minimum interstitial velocity for fines mobilisation is identified (Gruesbeck and Collins, 1982). This minimum interstitial velocity may very well be exceeded during CO_2 injection given the high CO_2 injection rates required at a CO_2 storage complex. Xie et al. (2017) used the DLVO (Derjaguin−Landau−Verwey−Overbeek) theory to describe the mobilisation of fines and argued that the fines were kaolinite particles detached from other kaolinite particles rather than quartz grains as typically explained in the oil industry (e.g. Rosenbrand et al., 2015).

More specifically for CO_2 injection and two-phase flow, Huang et al. (2018) and Aramrak et al. (2011) showed mathematically that the wettability of fine particles affects the interfacial force acting on a fine particle and thereby determine the likeliness of particle mobilisation. Wettability is defined as the tendency of a fluid to spread out on a surface in the presence of another fluid (McPhee et al., 2015) and is typically measured by the contact angle θ between the surface of the formation water and the fine particle. The lower the contact angle, the more water-wet the minerals are classified.

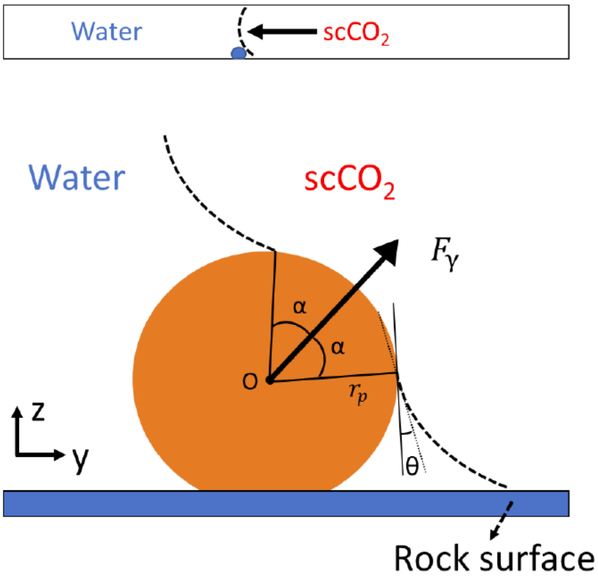

Figure 4.7 Interfacial force acting on a fine particle in the CO_2-water interface (Zhang et al., 2019).

Figure 4.7 shows the interfacial for acting on a fine particle in the CO_2-formation water interface. The higher the interfacial force, the larger potential for the particle to detach from the rock surface and enter the supercritical CO_2 phase. The interfacial force (F_γ) on a fine particle in the CO_2-formation water interface can be calculated by (Huang et al., 2018):

$$F_\gamma = 2\pi r_p \sin(\alpha) \sin(\theta-\alpha) \qquad (4.16)$$

where r_p is the particle radius, γ is the surface tension, θ is the contact angle and α is the filling angle which defines the position of the particle at the interface. Equation 4.16 clearly demonstrates that the interfacial force depends on the wettability (contact angle θ). Zhang et al. (2019) showed that for a given particle (with radius r_p), the maximum interfacial force acting on a particle is solely dependent on the contact angle, i.e. the wettability, which led the authors to conclude that CO_2-wet or neutral wet fines are more likely to be mobilized than water wet fines. Thus, microcline and muscovite are more potential to be mobilised at the CO_2-brine interface than quartz, chlorite, and kaolinite (Zhang et al, 2019).

Several authors suggest a strong influence of chemical reactions on fines migration (Dawson et al., 2015; Jean et al., 2015; Pudlo et al., 2015; Tang et al., 2016; Othman et al., 2018). For example, Othman et al., (2018) observed a significantly larger reduction in the permeability after $scCO_2$ injection compared to the reduction observed by Mohamed et al. (2012) and explained this difference with the fact that the latter did not inject CO_2-saturated brine before continuous $scCO_2$ injection. The low pH of the CO_2-saturated brine will react with the cementing material thereby creating fines that may migrate and reduce the permeability. The mixing of CO_2 and brine has been shown to be too slow to occur in a short dynamic experiment (Zhang et al., 2015) and Othman et al. (2018) therefore argued that during core flooding experiments, sandstone core samples should first receive injection of brine, then of CO_2-saturated brine, and finally of $scCO_2$. This series of injections may also be closer to a realistic scenario during CO_2 injection at a geological site.

The proposed mechanism for particle mobilisation during CO_2 sequestration is as follows: Part of the injected CO_2 dissolves in the formation water thereby decreasing the pH of the formation water surrounding the injected CO_2. This low-pH water can dissolve intergranular cement, which generates fines. As CO_2 injection continues, the injected CO_2 displaces the low-pH water laterally, away from the injection well. When the CO_2-brine interface passes over the generated fines, the interfacial force can displace the fines along the flow direction (Huang et al., 2018; Othman et al., 2018b). Injection stops, either due to periodically maintenance purposes or unintentionally shut-ins, may temporarily reverse the pressure gradient in the reservoir and potentially create conditions where fines can migrate towards the injection well. If the fines migrate into the sand control completion in the injection well, the fines may clog the pores of the sand control thereby reducing the fluid conductivity. How likely this scenario is will depend on pressure gradient history, completion choice and operation conditions (Torsætter and Cerasi, 2018). Discontinuous, cyclic injektion of CO_2 may thus cause challenges, that need to be considered in the context of a specific site. We therefore recommend that the potential for fines migration in the Gassum sandstone formation due to CO_2 injection be studied in a series of laboratory experiments.

5. Laboratory experiments

Changes in the chemical properties of the reservoir rock and the mechanisms responsible for these changes are typically characterised by laboratory experiments reproducing the conditions of CO_2 storage. These laboratory experiments also provide input data for predictive modelling. While the methods applied for characterising the initial properties of the reservoir (e.g. reservoir injectivity and storage potential) prior to CO_2 injection to a large extent are similar to those routinely performed in the oil and gas industry during the exploration of hydrocarbon reservoirs, characterising geochemical changes in the reservoir are far more challenging.

Several different experimental techniques exist, e.g. batch and flow-through experiments. No single approach can be considered a universal best analogue to test chemical reactions during injection and subsequent storage because of the range of settings in which reactions are possible within even a simple storage site and the range of injection scenarios that might be implemented. It is, however, crucial to design the laboratory experiment to give answers to the specific scientific questions one tries to answer. As illustrated in section 4, different CO_2-water-rock interactions take place in different parts of the CO_2 storage system. It is important that laboratory experiments relevant for geological CO_2 storage address all these settings, although most experiments have been designed to measure dissolution rates at far-from-equilibrium conditions.

The chemical effects of CO_2 storage are preferably determined in the laboratory using core specimen of samples cored while drilling the injection wells for the CO_2 storage site. Alternatively, samples taken from analogues considered similar to the rock material in the reservoir may be used. In either case, it is important to keep in mind that laboratory experiments typically use core samples of some cubic centimetres in volume and therefore the representativeness of the results relies on the quality of the sample. The representativeness of the sample depends on two main factors: the spatial heterogeneity of the studied geological unit and the care taken during sampling in order to minimize the alteration of the reservoir properties. A critical step of the experimental design is therefore the choice of samples as well as the number of samples and measurements needed to elucidate the scientific questions the laboratory is meant to provide answers to.

The following sections give an overview of the experimental techniques used for investigating chemical reactions between the water-CO_2 mixture flowing in the pore space and the rock-forming minerals and some of the challenges related to high-pressure experiments involving CO_2. The same techniques may be used for investigating the chemical effects of CO_2 storage on the cap rock and on well cement material.

5.1. Batch experiments

Batch experiments are standard techniques using static reactors (batch reactors) to typically study reaction kinetics under controlled conditions. A batch reactor is a heated vessel in which reactants are placed and reactions are allowed to proceed for a given time. This type of equipment is relatively simple and generally free from day-to-day maintenance. Consequently, it is well suited for running over prolonged periods. The batch experiments involve brine and/or CO_2 and powdered (to provide the maximum surface area for reaction) single minerals or multi-mineral rock, rock chips or rock samples. The experiments are designed for periodic sampling of the fluid for analysis and may be used to find reaction rate constants, activation energy and to determine the order of the reactions. From a thermodynamic point of view, a batch reactor represents a closed system and the system will tend to thermodynamic equilibrium with time.

Several different configurations exist for batch experiments including a simple tube equipped at one end by a CO_2 inlet with close off valve and at the other end a pressure release valve set at a given pressure. More sophisticated types of reactor are often used to improve the sampling or the control of the fluid composition, an example of which is shown in Figure 5.1.

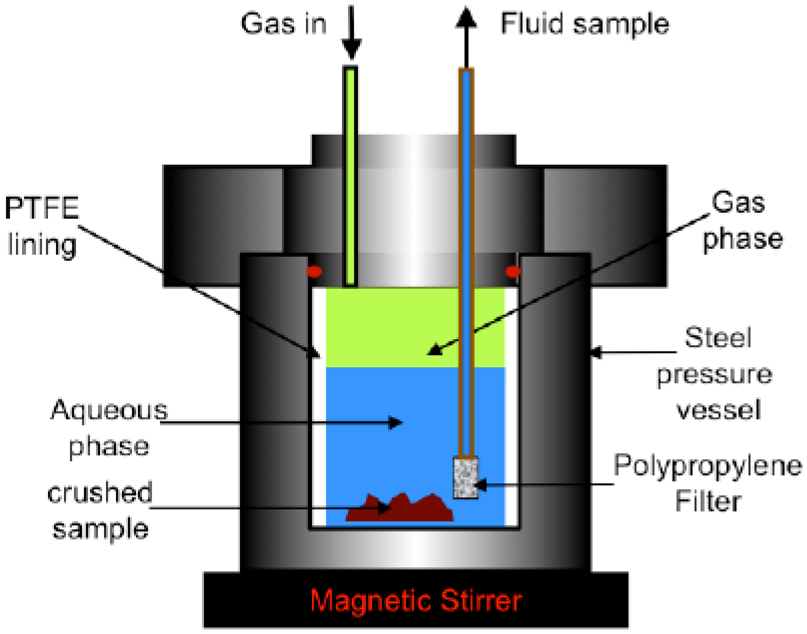

Figure 5.1 Schematic diagram of a typical batch reactor. From (Bateman and Purser, 2010)

5.2. Core flooding experiments

In flow-through experiments, a fluid is injected at a controlled rate through a reservoir sample, usually of cylindrical shape, called a plug. The fluid may be either a single-phase fluid, such as CO_2-rich brine, or a mixture of phases e.g. brine and $scCO_2$. The duration of these dynamic experiments is typically weeks. The experiments are suitable for determining time-elapsed changes of the sample properties such as permeability and porosity and to measure chemical reaction rates in dynamic conditions.

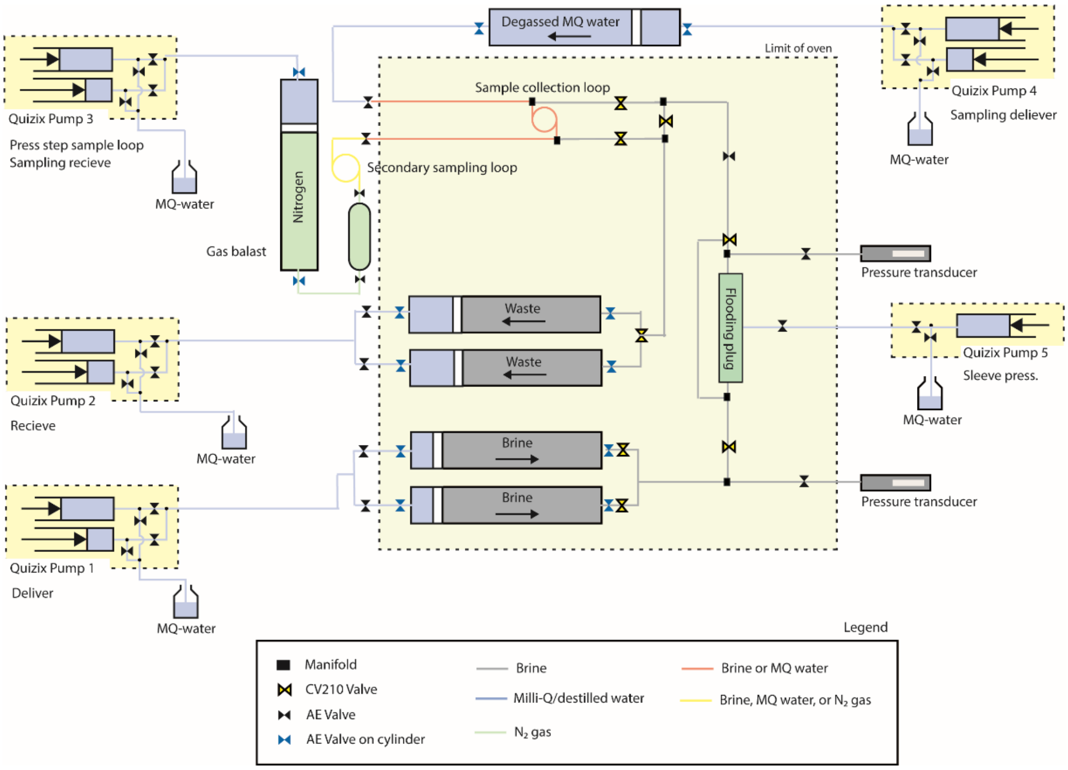

Figure 5.2: Experimental set up of a flow-through experiment as performed at the GEUS core laboratory.

A schematic representation of a flow-through experiments is shown in Figure 5.2. The system includes computer controlled two piston pumps that can deliver puls free flow with large accuracy, a core holder where the sample is installed and pressurised, an oven to control the temperature, and a back pressure system allowing control of the outlet pressure while permitting the fluid to be withdrawn from the circuit and sampled for chemical analysis. Several techniques exist for controlling the pressure of the system, e.g. the use of a back-pressure regulator or as shown in Figure 5.2 the use of a back-pressure piston pump. In the latter case a two-piston pump is programmed to maintain the desired pressure by continuously adapting the pistons displacement.

5.3. Materials for experimental apparatus

The experimental apparatus must be designed to span a wide range of pressure, temperature, and pCO_2 conditions. Particularly for experiments conducted with high pCO_2 and high-salinity brines, that are extremely corrosive due to the low pH and high salinity, the experimental apparatus should be constructed of inert materials so as not to participate in the reactions of interest. Usually corrosion resistant alloys such as Hastelloy are used at least for the most exposed parts such as pumps, tubing, and valves.

5.4. Sampling and pH measurement

A major challenge for high-pressure experiments involving CO_2 is sampling of the fluid for chemical analysis during the experiment. Special care should be taken during sampling to prevent degassing of CO_2. Degassing of CO_2 will affect the measurement of pCO_2 and pH which may affect the modelled chemical reaction rates and equilibrium states as these are highly pH dependent. In addition, degassing can cause formation of carbonates during sampling, which could result in erroneous determination of the concentration of dissolved Ca, Mg and Fe(II).

Many studies with CO_2 still measure pH as quickly as possible after reducing pressure to ambient pressure and rely on geochemical models to calculate pH at in situ conditions. However, recently electrodes have been developed to allow pH determinations at elevated pressure and temperature in experimental systems. Corr Instrument for instance provides a glass-based pH probe rated for temperatures up to 80°C and pressures up to *c.* 200 bar that could meet the experimental conditions for CO_2 storage laboratory experiments. Such a pH electrode is, however, currently not available at GEUS.

6. Geochemical modelling

A reasonable aim for geochemical modelling for CO_2 storage is outlined by the International Organization for Standardization (ISO 27914:2017). For the storage unit, it prescribes that modelling should evaluate short- and long-term geochemical changes occurring in the storage formation with respect to CO_2 trapping, the modifications that reactions might cause to porosity and permeability, and the impact of assumptions and uncertainties on predictions.

This is no simple task. Geochemical processes occur at the scale of atoms and results in physical changes at the scale of pores, yet we want to understand the outcome at much larger scale. Some processes, such as coupled nucleation and growth, can take considerable time before they commence, but when they occur, they proceed quickly; ideally, we want to capture such behaviour as we predict evolution over millennia. The geochemical processes are often intricately coupled with fluid flow; flow transports reactants and products, impacting reaction rates, but it is itself sensitive to the changes in pore geometry caused by the geochemical process it nourishes. The chemical and petrophysical properties of the formation rock varies in space, causing heterogeneities at different scale with impact on fluid flow and geochemical processes. Finally, many of the parameters required for the modelling are highly uncertain so that extensive sensitivity analysis is needed. Combined, this means that the problem at hand is such that it cannot simply be solved by brute computational force.

To circumvent this problem, different modelling methods are used at different spatial and temporal scale. Quantum mechanical modelling, such as those based on density functional theory, can derive interaction potentials for atoms, which can then be applied in molecular dynamics modelling to understand behaviour at the scale of thousands of atoms. Such theoretical modelling has been applied to understand $CaCO_3$ nucleation (Wallace et al., 2013) and CO_2 wettability (e.g., Liang et al., 2017; Silvestri et al., 2017). In the context of assuring the performance of a CO_2 storage site in Denmark, such modelling is most likely not required.

At the pore scale, modelling is performed to determine the discrete spatial position of phases (CO_2, water, and solid) and their evolution in time at fine spatial resolution, using either an actual pore space geometry or, to decrease computational costs, an extracted and simplified virtual representation (e.g., Steefel et al., 2013; Xiong et al., 2016). Fluid flow is typically computed using Navier-Stokes equation, lattice Boltzmann methods or particle methods. In pore scale modelling, the typical aim is to 1) derive results that represent larger volumes of rock, entailing that modelled systems are rather large and computational costly (Steefel et al., 2013), so that one can 2) assess either qualitatively or quantitatively how changes at the pore scale can influence the macroscopic properties of the rock such as permeability. Examples of such modelling include efforts to understand the details of two phase flow (e.g., Blunt et al., 2013; Ferrari and Lunati, 2013), the effect of flow on dissolution reactions (Kang et al., 2010; Molins et al., 2012; Nogues et al., 2013), the change in morphology of dissolving grains in flowing water (Dutka et al., 2020), mobility of particles dislodged by dissolution (Liu et al., 2020), coupled dissolution and precipitation of carbonates (Pedersen et al., 2016), and the changes occurring to well cement during interaction with CO_2 charged water (Raoof et al., 2012).

Clearly, such theoretical modelling has proven useful for understanding the physical evolution of the pore space caused by geochemical reactions. Compared to experiment, the modelling can be less time consuming, in particular if aspects of the model can be applied to study several types of processes. One might envision that a reasonably representative pore scale model of the Gassum formation could be applied to study residual trapping, colloidal transport, and the influence on permeability of mineral precipitation, which could be induced by drying, impurities in the CO_2, and by mineral carbonation during fingering. For pore scale geochemical modelling, however, studies have largely focused on dissolution reactions and much less on the coupled process of nucleation and growth, which occur when new mineral form. Although nucleation and growth of minerals have a high potential for changing fluid flow, only two published studies exist to our knowledge (Prasianakis et al., 2017; Fazelli et al., 2020). There might be several reasons for this: 1) Nucleation is occurring at very short time scales and the nucleus is extremely small, which means that it is exceptionally complicated to observe the phenomenon and provide accurate data for modelling. 2) It is likely to occur heterogeneously at minute irregularities on the surface of existing minerals; these irregularities are too small for direct observation and their characteristics, density and location would have to be inferred from other types of data. 3) Within classical theory, nucleation occurs probabilistically, adding a layer of complexity to the computation (Fazelli et al., 2020). 4) The interfacial tension of the nuclei, which is required for modelling of nucleation, is poorly constrained. To conclude, modelling of nucleation and growth is challenging, but it could well give critical understanding of the impact geochemical reactions have on fluid mobility.

Because of the size and time scale of CO_2 storage, the bulk of the geochemical calculation inevitably relies on continuum modelling. Here, the locally heterogeneous properties of the rock are averaged to give representative volumes that are described in macroscopic terms such as porosity, permeability, average composition and specific surface area. Fluid flow is typically computed using Darcy's law (Sin and Corvisier, 2019), and quantification of mineral-water reactions usually rely on equilibrium or reaction rates (expressions similar to equations 4.1-4.5) Numerous examples of such modelling exist. It has provided information on the flow rates during the density driven flow of CO_2 charged water (fingering) and the temporal evolution of solubility trapped CO_2 (e.g., Preuss and Zhang, 2008; Pau et al, 2010); the effect of injection of liquid CO_2 (Vilarrasa et al., 2013); the extent of mineral carbonation (e.g., Audigane et al., 2007) and the geochemical impact of impurities in CO_2 (e.g., Xu et al., 2007; Tokada and Xu, 2017; Spycher et al., 2019). Clearly, continuum based geochemical modelling can provide information critical to the outcome of CO_2 storage, including calculation of the time scales of CO_2 dissolution and formation of carbonates. Assuming that the temporal evolution of the CO_2 trapping mechanisms has to be assessed for a given storage site, continuum modelling would be indispensable.

The knowledge gained from pore scale and continuum modelling becomes truly valuable, when results can be translated from the pore scale to the scale at which reservoirs are modelled and vice versa. Although this translation is far from straight forward, a range of methods exists from decades of research (Molins and Knabner, 2019). Examples include calibration of the parameters used in continuum modelling from pore scale modelling (e.g., Nogues et al., 2013; Varloteaux et al., 2013) and models capable of performing pore scale modelling in certain regions and coupling the outcome to a general continuum modelling (e.g. Balhoff et al., 2008; Scheibe et al., 2015).

For a Danish storage formation, multiscale modelling could be applicable for the study of several regions where geochemical reactions are intimately coupled to fluid flow or could have significant consequences for flow. The simple 1D reactive transport modelling performed to survey the effect of impurities indicated that substantial amounts of mineral transformation could occur where water was close to impure supercritical CO_2. It would be prudent to survey if new formed materials would be likely to form at pore throats, which could impart permeability adversely. Similarly, the mineral carbonation during fingering may be sufficiently fast to change the permeability during fingering. To test if this is the case and to understand the consequences for the temporal evolution of CO_2 trapping, multiscale modelling could also be performed. In addition, multiscale modelling of drying could also be important to assess if permeability could decrease in the vicinity of the injection well. All types of studies would require pore scale modelling of nucleation and growth, which most likely would be complicated. However, results from the pore scale could be embedded in a continuum scale description of the processes, which we have already developed for the geochemical software PHREEQC to describe barite nucleation in wells (manuscript in progress). Thus, we might already have one of the pieces for the puzzle.

7. Recommendation for future research

7.1 Mineralogy and reservoir quality

Reservoir mineralogy is essential for the chemical reactions that may occur when the reservoir is exposed to CO_2, so it is important to make good estimates of the mineralogy prior to CO_2 injection. The mineralogy is also important for the reservoir quality because the reservoir properties are dependent on the diagenetic processes. Thus, diagenesis modelling is recommended to estimate the mineralogy, porosity and permeability of the reservoir in areas without well information. A diagenesis model has been created for the Gassum Formation using the Touchstone software by performing forward diagenesis modelling of the evolution in mineralogy and reservoir quality. The petrographic input data comprise the composition of detrital and authigenic phases, the grain-coat coverage and the grain size. The reservoir property input data include unstressed porosity, permeability and density measurements besides a subset of stressed analyses. The burial history input data comprise the evolution in depth, temperature and effective stress.

To improve the diagenesis model, more analyses of reservoir properties at reservoir pressure conditions are recommended to understand how the pressure affects especially permeability during burial. It is also proposed to perform more in situ stable isotope analyses of authigenic cement types and other mineralogical temperature indicators that can help constrain the burial history. For every new deep well drilled in Denmark, it is recommended to take cores and subject the reservoir intervals to petrographic analysis including mineral quantification and to carry out core analysis with measurement of porosity and permeability. Vitrinite reflectance analysis of new core material is also advised to improve the local burial history. All these data can then be used to constrain the diagenesis model further.

The diagenesis model that has been established for the Gassum Formation can be used to make qualified pre-drill estimates of mineralogy and reservoir properties if local and regional variations are thoroughly considered. Similarly, the establishment of a diagenesis model for the Skagerrak and Bunter Sandstone Formations would give important insights about where this reservoir has properties that are appropriate for CO_2 storage, so the creation of such a model is recommended.

The results of the diagenesis modelling including reservoir quality prediction by Touchstone software at potential well locations can be extended onto map surfaces using T>Map software by incorporating 3D basin modelling, burial histories and facies distributions. By taking the temperature- and facies-dependence of the different diagenetic processes into account, the spatial distribution of the reservoir properties can be simulated for an entire sandstone reservoir along each of its prominent surfaces, which are identified by sequence stratigraphic correlation and seismic mapping. This approach is recommended for future studies for each relevant reservoir.

Development of a machine learning approach in the mineralogical quantification of detrital and authigenic phases is recommended. Such an automated procedure will have several important advantages such as information of the specific chemistry for the analysed minerals and removal of the operator bias associated with mineral identification. Mineralogical quantification of sandstone is traditionally made by point counting of thin sections during optical microscopy where a petrographer identifies the phases present in the sandstone. Automated mineral quantification can be made by scanning electron microscopy (SEM), but the distinction between detrital and authigenic minerals can currently only be made by operators, and this information is of utmost importance when evaluating the diagenetic history and reservoir quality of a sandstone. A Field Emission SEM with an optimal combination of detectors can be used to test if machine learning can train a software to be able to make a distinction between detrital and authigenic minerals.

7.2 Hydrogeochemical reactions

The rate and extent of the above described chemical reactions determining the fate of CO_2 in a geological storage site are highly dependent on local conditions such as reservoir mineralogy, formation water chemistry, reservoir pressure and temperature. Therefore laboratory experiments using site specific core material and geochemical modelling using site specific data are necessary to better predict the fate of CO_2 in these structures specifically. Especially the mineralogy of the Havnsø structure is currently related with large uncertainties and new core material from this structure is highly recommended to be able to predict the fate of CO_2 in this structure. However, since core material from either of the two structures are currently not available, general conclusions may be drawn using analogue core material in laboratory experiments to increase our hydrogeochemical knowledge related to CO_2 storage which may help identifying possible future Danish CO_2 storage sites. Likewise, geochemical models using data from analogue locations will be a valuable tool for maturation of a possible prospect before site specific data are available. Such calculations would, for example, allow us to estimate the impact of uncertainties on predictions.

Laboratory based studies give results that reflect all the processes occurring in the experiments. Thus, it provides a picture that is far more complete and complex than the simplified representation of reality, which computational modelling offers. However, experimental work is costly in terms of person hours and equipment and the obtained information is specific to the experimental setup and the conditions selected. Hence, it is often most effective if performed when scientific questions can be specific and well posed. Geochemical modelling can help us define these questions.

Our understanding of how geochemical reactions could unfold in the storage formation upon CO_2 injection is currently limited by several factors; we can hypothesize the occurrence of a variety of reactions at various locations in the formation, but we cannot at the moment safely identify which could have most critical impact on the operation because several central parameters are unknown. Most importantly these include the amount of CO_2 injected, its composition and temperature, and the injection rate over time. If the injected CO_2 is saturated with water, for example, we would not need to concern ourselves with drying of the rock; if pure, we can neglect the impact of impurities.

Combined with existing knowledge, realistic estimates of the nature and amounts of injected CO_2 would allow us to conduct much more qualified reactive transport modelling that would pinpoint where, how and to what extend geochemical reactions could be detrimental or beneficial to the performance of the storage site. This modelling would also allow us to define critical unknowns that should be quantified experimentally and provide the basis for design of the experiment. The initial modelling will be performed while site specific core material is acquired. Thus, we propose a three stage plan for future work.

Stage 1. Initial reactive transport modelling to identify the overall behavior of the system, the nature and location of critical geochemical reactions, and the parameters that are unknown or highly uncertain. Given that the values for many of the input parameters will be uncertain at this point, extensive sensitivity analysis will have to be performed. Because such analysis will be computationally expensive, other aspects of the model will have to be simplified, such as the spatial resolution and the number of processes modelled simultaneously. Such a screening by modelling allows us to recognize what types of additional information are required and design the experiments accordingly. This initial work would also allow us to extend our modelling competences into multidimensional reactive transport modelling so that we become more familiar with the computational codes designed explicitly for advanced reactive transport modelling (e.g., TOUGHREACT; Xu et al., 2011; and STOMP; Kim et al., 2014), or those that are designed for transport, but can be coupled to other software for the reactive part (e.g., COMSOL and PHREEQC, Sainz-Garcia et al., 2017; Dumu^X and PHREEQC; Koch et al., 2020).

For a Danish storage formation, multiscale modelling could be applicable for the study of several regions where geochemical reactions are intimately coupled to fluid flow or could have significant consequences for flow. Given that this work would most likely focus on identifying the location of new formed phases, it would entail pore scale modelling of nucleation and growth. This would be a challenging task that could require calibration of the model with experimental observation of the spatial distribution of secondary phases as a function of time using in-situ X-ray tomography or similar techniques.

Activities during Stage 1 include: 1) Tests or development of methods to accurately describe the thermodynamic properties at reservoir conditions of aluminosilicates (and possibly other groups of minerals, whose description we are currently testing). 2) Tests of methods to describe the change in mineral reactivity as a function of time so that we can translate reaction rates obtained in laboratory to those occurring in the field. 3) Defining the uncertainty range for all parameters used in the modelling. 4) Benchmarking of the performance of several computational codes with a focus on their capabilities for modelling the coupling of flow and geochemical reactions. Potential field data for comparison with modelled results include that from the storage of natural gas at Stenlille. For benchmarking the pore scale modelling, data may well have to be generated within the project. 5) Development of models for the storage formation and tests of their performance and the influence of geological heterogeneities. 6) Actual modelling to obtain the required information. We estimate that this work will take place over 1-2 years.

Stage 2. Experimental work to provide the information required for correct modelling of the critical processes, making use of the experimental approaches described above as well as novel methods if needed. Site specific core material should be used for the laboratory experiments and the material should be thoroughly characterised before and after experiments using techniques such as optical microscopy, X-ray diffraction and scanning electron microscopy coupled with energy dispersive X-ray spectroscopy, including mineralscan. In addition, X-ray tomography could also be applied.

We estimate that the experimental work will span over 2 years, given the long duration of each experiment.

Stage 3. Elaborate reactive transport modelling using the knowledge gained in Stage 1 and 2 and during site characterisation to quantify the impact of geochemical reactions on the performance of the storage facility. If sufficient information has been obtained from site characterisation, this modelling should provide the results outlined by the International Organization for Standardization (ISO 27914:2017), setting the stage for operation. The work will include substantial sensitivity analysis to firmly define uncertainties in the outcomes. We estimate that the Stage 3 modelling can be completed in 1 year, because models have already been established in Stage 1.

8. References

Al-Yaseri, A., Zhang, Y., Ghasemiziarani, M., Sarmadivaleh, M., Lebedev, M., Roshan, H., Iglauer, S., 2017. Permeability evolution in sandstone due to CO_2 injection. Energy Fuels 31, 12390–12398.

Aminu, M.D, Nabavi, S.A, Rochelle, C.A., Manovic, V., 2017. A review of developments in carbon dioxide storage. Applied Energy 208, 1389-1419.

André, L., Audigane, P., Azaroual, M., Menjoz, A., 2007. Numerical modelling of fluid–rock chemical interactions at the supercritical CO_2–liquid interface during supercritical CO_2 injection into a carbonate reservoir, the Dogger aquifer (Paris Basin, France). Energy Conversion and Management 48, 1782–1797.

Anthonsen, K.L., Frykman, P., Nielsen, L.H., 2011. The potential for geological storage of CO_2 in Denmark is very promising. In: Sønderberg Petersen, L., Larsen, H. (eds): Energy Systems and Technologies for the Coming Century: Proceedings.

Anthonsen, K.L., Nielsen, C.M., Kristensen, L., Laier, T., Johannessen, P., 2019. CO_2 Neutral energy system utilising the subsurface. Geological Survey of Denmark and Greenland report 2019/21, 55 pp.

API, 1998. American Petroleum Institute, API RP 40, Recommended Practice for Core Analysis, 2nd edn. American Petroleum Institute, Washington, DC.

Appelo, C.A.J. and Postma, D., 2005. Geochemistry, groundwater and pollution, 2nd ed. A. A. Balkema Publisher.

Aramrak, S., Flury, M., Harsh, J. B., 2011. Detachment of deposited colloids by advancing and receding air-water interfaces. Langmuir 27, 9985–9993

Audigane, P., Gaus, I., Czernichowski-Lauriol, I., Pruess, K., Xu, T., 2007. Two-dimensional reactive transport modeling of CO_2 injection in a saline aquifer at the Sleipner site, North Sea. American Journal of Science 307, 974-1008.

Azaroual, M., Pruess, K., Fouillac, C., 2007. Feasibility of using supercritical CO_2 as heat transmission fluid in the EGS (Enhanced Geothermal Systems) integrating the carbon storage constraints. In: ENGINE – Enhanced Geothermal Innovative Network for Europe. Workshop 2: exploring high temperature reservoirs: new challenges for geothermal energy, SIAF Campus, Volterra, Italy, 1–4 April.

Bachu, S., 2003. Screening and ranking of sedimentary basins for sequestration of CO_2 in geological media in response to climate change. Environmental Geology 44, 277–289.

Bachu, S., Adams, J.J., 2003. Sequestration of CO_2 in geological media in response to climate change: capacity of deep saline aquifers to sequester CO_2 in solution. Energy Conversion and Management 44, 3151–3175.

Balhoff, M., Thomas, S. G., Wheeler, M. F., 2008. Mortar coupling and upscaling of pore-scale models. Computers and Geosciences 12, 15-27.

Bateman, K. and Purser, G., 2010. Geological storage of CO_2 in the Danish Underground: Evaluation of the response of the reservoir and cap rocks to CO_2. British Geological Survey External Report, CR/10/153. 27 pp.

Bertelsen, F., 1978. The Upper Triassic–Lower Jurassic Vinding and Gassum formations of the Norwegian-Danish Basin. Geological Survey of Denmark series B, 3, 1–26.

Blunt, M.J., Bijeljic, B., Dong, H., Gharbi, O., Iglauer, S., Mostaghimi, P., Paluszny, A., Pentland, C., 2013. Pore-scale imaging and modelling. Advances in Water Resources 51, 197–216.

Burnside, N.M., Naylor, M., 2014. Review and implications of relative permeability of CO_2/brine systems and residual trapping of CO_2. International Journal of Greenhouse Gas Control 23, 1–11.

Civan, F. 2007: Reservoir formation damage. Fundamentals, modelling, assessment and mitigation. 2nd Edition. Elsevier Scientific Publishing Co.

Dawson, G., Pearce, J., Biddle, D., Golding, S., 2015. Experimental mineral dissolution in Berea Sandstone reacted with CO_2 or SO_2-CO_2 in NaCl brine under CO_2 sequestration conditions. Chemical Geology 399, 87–97.

Dutka, F., Starchenko, V. Osselin, F., Magnia, S., Szymczak, P., Ladd, A. J. C., 2020. Time-dependent shapes of a dissolving mineral grain- Comparisons of simulations with microfluidic experiments. Chemical Geology 540, 119459.

Erlström, M., Boldreel, L.O., Lindström, S., Kristensen, L., Mathiesen, A., Andersen, M.S., Kamla, E., Nielsen, L.H., 2018. Stratigraphy and geothermal assessment of Mesozoic sandstone reservoirs in the Øresund Basin – exemplified by well data and seismic profiles. Bulletin of the Geological Society of Denmark 66, 123–149.

Eveloy, V., Gebreegziabher, T., 2018. A review of projected Power-to-Gas deployment scenarios. Energies 11, 1824.

Fazeli, H., Masoudi, M., Patel, R.A., Aagaard, P., Hellevang, H., 2020. Pore-Scale Modeling of nucleation and growth in porous media. ACS Earth Space Chemistry. 4, 249−260.

Ferrari, A., Lunati, I., 2013. Direct numerical simulations of interface dynamics to link capillary pressure and total surface energy. Advances in Water Resources 57, 19–31.

Friis, H., 1987. Diagenesis of the Gassum Formation, Rhaetian-Lower Jurassic, Danish Subbasin. Geological Survey of Denmark series A, 18, 1–41.

Fuchs, S., Balling, N., Mathiesen, A., 2020. Deep basin temperature and heat-flow field in Denmark – new insights from borehole analysis and 3D geothermal modelling. Geothermics 83, 101722.

Gaus, I., Audigane, P., André, L., Lions, J., Jacquemet, N., Durst, P., Czernichowski-Lauriol, I., Azaroual, M., 2008. Review: Geochemical and solute transport modelling for CO_2 storage, what to expect from it? International Journal of Greenhouse Gas Control 2, 605–625.

Gluyas, J., Cade, C.A., 1997. Prediction of porosity in compacted sands. In: Kupecz, J.A., Gluyas, J., Block, S. (eds): Reservoir quality prediction in sandstones and carbonates. American Association of Petroleum Geologists Memoir 69, 19–28.

Gregersen, U., Vosgerau, H., Laghari, S., Bredesen, K., Rasmussen, R., Mathiesen, A., 2020. Capture, Storage and Use of CO_2 (CCUS): Seismic interpretation of existing 2D and 3D seismic data around the Havnsø structure (Part of work package 5 in the CCUS project). Geological Survey of Denmark and Greenland report 2020/33, 60 pp.

Gruesbeck, C., Collins, R.E., 1982. Entrainment and deposition of fine particles in porous media. SPE Journal 22, 10

Hjelm, L., Anthonsen, K.L., Dideriksen, K., Nielsen, C.M., Nielsen, L.H., Mathiesen, A., 2020. Capture, Storage and Use of CO_2 (CCUS): Evaluation of the CO_2 storage potential in Denmark (Part of work package 5 in the CCUS project). Geological Survey of Denmark and Greenland report 2020/46, 60 pp.

Hjuler, M.L., Vosgerau, H., Nielsen, C.M., Frykman, P., Kristensen, L., Mathiesen, A., Bidstrup, T., Nielsen, L.H., 2014. A multidisciplinary study of a geothermal reservoir below Thisted, Denmark. Geological Survey of Denmark and Greenland Bulletin 31, 51–54.

Holmslykke, H.D., Kjøller, C., Fabricius, I.L., 2017. Core flooding experiments and reactive transport modeling of seasonal heat storage in the hot deep Gassum Sandstone Formation. ACS Earth and Space Chemistry 1(5), 251–260.

Holmslykke, H.D., Schovsbo, N.H., Kristensen, L., Weibel, R., Nielsen, L.H., 2019a. Characterising brines in deep Mesozoic sandstone reservoirs, Denmark. Geological Survey of Denmark and Greenland Bulletin 43, e2019430104.

Holmslykke, H.D., Weibel, R., Hedegaard, K., Karan, S., Rosenbom, A.E., 2019b. Investigating the discrepancy between gas and liquid permeability in the Gassum and Skagerrak Formations. Geological Survey of Denmark and Greenland report 2019/25, 38 pp.

Huang, F., Kang, Y., You, L., Li, X., You, Z., 2018. Massive fines detachment induced by moving gas-water interfaces during early stage two-phase flow in coalbed methane reservoirs. Fuel 222, 193–206.

Ilgen, A.G., Cygan, R.T., 2016. Mineral dissolution and precipitation during CO_2 injection at the Frio-I Brine Pilot: Geochemical modeling and uncertainty analysis. International Journal of Greenhouse Gas Control 44, 166–174.

IPCC, 2005. IPCC Special Report on carbon dioxide capture and storage. Prepared by Working Group III of the Intergovernmental Panel on Climate Change [Metz, B., Davidson, O., de Coninck, H.C., Loos, M., Meyer, L.A. (Eds.)]. Cambridge University Press, Cambridge, United Kingdom/ New York, NY, USA, 442 pp.

Jakobsen, R., 2020. Capture, Storage and Use of CO_2 (CCUS): CO_2 leakage and effects on the chemistry of aquatic systems – monitoring and remediation (Part of work package 7 in the CCUS project). Geological Survey of Denmark and Greenland report 2020/39, 28 pp.

Japsen, P., Bidstrup, T., 1999. Quantification of late Cenozoic erosion in Denmark based on sonic data and basin modelling. Bulletin of the Geological Society of Denmark 46, 79–99.

Japsen, P., Green, P.F., Nielsen, L.H., Rasmussen, E.S., Bidstrup, T., 2007. Mesozoic–Cenozoic exhumation events in the eastern North Sea Basin: a multi-disciplinary study based on palaeothermal, palaeoburial, stratigraphic and seismic data. Basin Research 19, 451–490

Jean, J.S., Wang, C.L., Hsiang, H.I., Li, Z., Yang, H.J., Jiang, W.T., Yang, K.M., Bundschuh, J., 2015. Experimental investigation of trace element dissolution in formation water in the presence of supercritical CO_2 fluid for a potential geological storage site of CO_2 in Taiwan. Journal of Natural Gas Science and Engineering 23, 304–314.

Johnson, M.R., 1994. Thin section grain size analysis revisited. Sedimentology 41, 985–999.

Kampman, N., Bickle M., Wigley, M., Dubacq, B., 2014. Fluid flow and CO_2-fluid-mineral interactions during CO_2-storage in sedimentary basins. Chemical Geology 369,22-50.

Kang, Q., Lichtner, P.C., Viswanathan, H.S., Abdel-Fattah, Amr I., 2010. Pore Scale Modeling of Reactive Transport Involved in Geologic CO_2 Sequestration. Transport in Porous Media 82, 197–213.

Kazmierczak, J., Marty, N., Holmslykke, H.D., Weibel, R., 2019. The risk of scaling and corrosion predicted formation water composition for Danish geothermal plants. Geological Survey of Denmark and Greenland report 2019/24, 54 pp.

Keiding, M., 2020. Capture, Storage and Use of CO_2 (CCUS): Geophysical methods to monitor injection and storage of CO_2 (Part of work package 7 in the CCUS project). Geological Survey of Denmark and Greenland report 2020/40, 31 pp.

Khilar, K.C., Fogler, H.S., 1983. Water Sensitivity of Sandstone. SPE 10103.

Khilar, K.C., Fogler, H.S., 1998. Migrations of fines in porous media. Springer Science & Business Media.

Kim, J., Sonnenthal, E., Rutqvist, J.A., 2015. A sequential implicit algorithm of chemo-thermo-poro-mechanics for fractured geothermal reservoirs. Computers & Geosciences 76, 59-71.

Koch, T., Gläser, D., Weishaupt, K., Ackermann, S., Beck, M., Becker, B., Burbulla, S., Class, H., Coltman, E., Emmert, S., Fetzer, T., Grüninger, C., Heck, K., Hommel, J., Kurz, T., Lipp, M., Mohammadi, F., Scherrer, S., Schneider, M., Seitz, G., Stadler, L., Utz, M., Weinhardt, F., Flemisch, B., 2020. DuMux 3 – an open-source simulator for solving flow and transport problems in porous media with a focus on model coupling, Computers & Mathematics with Applications. https://doi.org/10.1016/j.camwa.2020.02.012.

Kristensen, L., 2020. Capture, Storage and Use of CO_2 (CCUS): Reservoir data – Stenlille area (Part of work package 6 in the CCUS project). Geological Survey of Denmark and Greenland report 2020/28, 55 pp.

Kristensen, L., Hjuler, M.L., Frykman, P., Olivarius, M., Weibel, R., Nielsen, L.H., Mathiesen, A., 2016. Predrilling assessments of average porosity and permeability in the geothermal reservoirs of the Danish area. Geothermal Energy 4 (6), 1–27.

Laier, T., 2008. Chemistry of Danish saline formation waters relevant for core fluid experiments: fluid chemistry data for lab experiments related to CO_2 storage in deep aquifers. Geological Survey of Denmark and Greenland Report 2008/48, 10 pp.

Laier, T., Øbro, H., 2009. Environmental and safety monitoring of the natural gas underground storage at Stenlille, Denmark. In: Evans, D.J., Chadwick, R.A. (eds): Underground gas storage: Worldwide experiences and future development in the UK and Europe. The Geological Society, London, Special Publications 313, 81–92.

Larsen, G., 1966. Rhaetic - Jurassic - Lower Cretaceous sediments in the Danish Embayment (a heavy-mineral study). Geological Survey of Denmark row 2, 91, 1–127.

Larsen, T.B., Voss, P.H., Dahl-Jensen, T., 2020. Capture, Storage and Use of CO_2 (CCUS): Seismology in relation to safe storage of CO_2 (Part of work package 7 in the CCUS project). Geological Survey of Denmark and Greenland report 2020/41, 28 pp.

Liang, Y., Tsuji, S. Jia, J., Matsuoka, T. 2017. Modeling CO_2−water−mineral wettability and mineralization for carbon geosequestration. Accounts of Chemical Research 50, 1530−1540.

Liu, M., Starchenko, V., Anovitz, L.M., Stack, A.G., 2020. Grain detachment and transport clogging during mineral dissolution in carbonate rocks with permeable grain boundaries. Geochimica et Cosmochimica Acta 280, 202–220.

Lund, H., Østergaard, P.A., Connolly, D., Ridjan, I., Mathiesen, B.V., Hvelplund, F., Thellufsen, J.Z., Sorknæs, P., 2016. Energy storage and smart energy systems. International Journal of Sustainable Energy Planning and Management 11, 3-14.

Major, M., Poulsen, S.E., Balling, N., 2018. A numerical investigation of combined heat storage and extraction in deep geothermal reservoirs. Geothermal Energy, 6 (1), 16 pp.

Mathiesen, A., Laghari, S., Rasmussen, R., 2020a. Capture, Storage and Use of CO_2 (CCUS): Depth conversion of seal and reservoir maps from the Havnsø and Hanstholm areas (Part of work package 5 in the CCUS project). Geological Survey of Denmark and Greenland report 2020/35, 43 pp.

Mathiesen, A., Larsen, M., Mahler, A., 2003. Feasibility of CO_2 storage in combination with geothermal plants, Denmark. Geological Survey of Denmark and Greenland report 2003/79, 30 pp.

Mathiesen, A., Nielsen, L.H., Vosgerau, H., Poulsen, S.E., Bjørn, H., Røgen, B., Claus Ditlefsen, C., Vangkilde-Pedersen, T., 2020b. Geothermal Energy Use, Country Update report for Denmark. Proceedings World Geothermal Congress 2020, Reykjavik, Iceland. 14 pp.

Mathiesen, B.V., Lund, H., Connolly, D., Wenzel, H., Østergaard, P.A., Möller, B., Nielsen, S., Ridjan, I., Karnøe, P., Sperling, K., Hvelplund, F.K., 2015. Smart Energy Systems for coherent 100% renewable energy and transport solutions. Applied Energy 145, 139-154.

Matter J. M., Stute M., Snæbjörnsdottir S. Ó., Oelkers E. H., Gislason S. R., Aradottir E. S., Sigfusson B., Gunnarsson I., Sigurdardottir H., Gunnlaugsson E., Axelsson G., Alfredsson H. A., Wolff-Boenisch D., Mesin K., Fernandez de la Reguera Taya D., Hall J., Dideriksen K. and Broecker W. S. (2016) Rapid carbon mineralization for permanent and safe disposal of anthropogenic carbon dioxide emissions. Science 352, 1312-1314.

McPhee C., Reed, J., Zubizarreta, I., 2015. Chapter 7 - Wettability and Wettability Tests. In: McPhee C., Reed, J., Zubizarreta, I (eds.) Developments in Petroleum Science. Elsevier.

Metz, B., Davidson, O., De Coninck, H., Loos, M., Meyer, L., 2005. Intergovernmental panel on climate change (IPCC) special report on carbon dioxide capture and storage. Cambridge University Press, UK.

Michelsen, O., Nielsen, L.H., Johannessen, P.N., Andsbjerg, J., Surlyk, F., 2003. Jurassic lithostratigraphy and stratigraphic development onshore and offshore Denmark. In: Ineson, J.R., Surlyk, F. (eds): The Jurassic of Denmark and Greenland. Geological Survey of Denmark and Greenland Bulletin 1, 147–216.

Molins, S., Knabner, P., 2019. Multiscale Approaches in Reactive Transport Modeling. Reviews in Mineralogy and Geochemistry 85, 27-48.

Molins, S., Trebotich, D., Steefel, C.I., Shen, C., 2012. An investigation of the effect of pore scale flow on average geochemical reaction rates using direct numerical simulation. Water Resources Research 48, W03527.

Morton, A.C., Hallsworth, C., 1994. Identifying provenance-specific features of detrital heavy mineral assemblages in sandstones. Sedimentary Geology 90, 241–256.

Muecke, T.W., 1979. Formation fines and factors controlling their movement in porous media. Journal of Petroleum Technology 31, 144–150.

Nielsen, L.H., 2003. Late Triassic-Jurassic development of the Danish Basin and Fennoscandian Border Zone, Southern Scandinavia. In: Ineson, J.R., Surlyk, F. (eds): The Jurassic of Denmark and Greenland. Geological Survey of Denmark and Greenland Bulletin 1, 459–526.

Nielsen, L.H., Japsen, P., 1991. Deep wells in Denmark 1935-1900. Lithostratigrafisk subdivision. Danmarks Geologiske Undersøgelse, DGU Serie A, 31, 179 pp.

Nogues, J.P., Fitts, J. P., Celia, M.A., Peters, C.A., 2013. Permeability evolution due to dissolution and precipitation of carbonates using reactive transport modeling in pore networks. Water Resources Research. 49, 6006–6021.

Oelkers, E.H., Gislason, S.R., Matter, J., 2008. Mineral Carbonation of CO_2. Elements 4(5), 333–337.

Olivarius, M., Balling, N., Baunsgaard, J.P.M., Dalgaard, E., Holmslykke, H.D., Mathiesen, A., Mathiesen, T., Vosgerau, H., Weibel, R., Nielsen, L.H., 2020a. Investigation of the geological, technical and economical obstacles for large-scale utilization of geothermal energy from Danish sandstone reservoirs. Display presentation at EGU General Assembly.

Olivarius, M., Heredia, B.D., Malkki, S.N., Thomsen T.B., Vosgerau, H., 2020b. Capture, Storage and Use of CO_2 (CCUS): Provenance of the Gassum Formation: Implications for reservoir distribution and mineralogy (Part of work package 6 in the CCUS project). Geological Survey of Denmark and Greenland report 2020/38, 35 pp.

Olivarius, M., Laier, T., Knudsen, C., Malkki, S.N., Thomsen, T.B., Serre, S.H., Kristensen, L., Willumsen, M.E., Nielsen, L.H., 2018a. Source and occurrence of radionuclides in geothermal water. With focus on the Margretheholm geothermal plant. Geological Survey of Denmark and Greenland report 2018/41, 77 pp.

Olivarius, M., Sundal, A., Weibel, R., Gregersen, U., Baig, I., Thomsen, T.B., Kristensen, L., Hellevang, H., Nielsen, L.H., 2019a. Provenance and sediment maturity as controls on CO_2 mineral sequestration potential of the Gassum Formation in the Skagerrak. Frontiers in Earth Science 7 (312), 23 pp.

Olivarius, M., Tremosa, J., Mathiesen, A., Weibel, R., Dalgaard, M.T., Nielsen, L.H., 2019b. Diagenesis modelling of the geothermal reservoir quality of the Gassum Formation sandstones. Geological Survey of Denmark and Greenland report 2019/23, 58 pp.

Olivarius, M., Vosgerau, H., Thomsen, T.B., Serre, S.H., Nielsen, L.H., 2018b. Radiometric age dating of detrital zircons from the Gassum Formation in Jylland. Geological Survey of Denmark and Greenland report 2018/45, 15 pp.

Othman, F., Wang, Y., Hussain F., 2018. The effect of Fines migration during CO_2 injection using pore scale characterization. SPE-192076-MS.

Ott, H., de Kloe, K., Marcelis, F., Makurat, A., 2011. Injection of supercritical CO_2 in brine saturated sandstone: pattern formation during salt precipitation. Energy Procedia 4, 4425–4432.

Parkhurst, D.L. and Appelo, C.A.J., 2013. Description of input and examples for PHREEQC version 3 - A computer program for speciation, batch-reaction, one-dimensional transport, and inverse geochemical calculations, U.S. Geological Survey Techniques and Methods.

Pasquinelli, L., Felder, M., Gulbrandsen, M.L., Hansen, T.M., Jeon, J.-S., Molenaar, N., Mosegaard, C., Fabricius, I.L., 2020. The feasibility of high-temperature aquifer thermal energy storage in Denmark: the Gassum Formation in the Stenlille structure. Bulletin of the Geological Society of Denmark 68, 133–154.

Pau, G.S.H., Bell, J.B., Pruess, K., Almgren, A.S., Lijewski, M.J., Zhang, K., 2010. High-resolution simulation and characterization of density-driven flow in CO_2 storage in saline aquifers. Advances in Water Resources 33, 443–455.

Pedersen, J. Jettestuen, E., Madland, M.V., Hildebrand-Habel, T., Korsnes, R.I., Vinningland, J.L., Hiorth, A., 2016. A dissolution model that accounts for coverage of mineral surfaces by precipitation in core floods. Advances in Water Resources 87, 68-79.

Petersen, H.I., Nielsen, L.H., Bojesen-Koefoed, J.A., Mathiesen, A., Kristensen, L., Dalhoff, F., 2008. Evolution of the quality, thermal maturity and distribution of potential source rocks in the Danish part of the Norwegian–Danish basin. Geological Survey of Denmark and Greenland Bulletin 16, 66 p.

Peysson, Y., Bazin, B., Magnier, C., Kohler, E., Youssef, S., 2011. Permeability alteration due to salt precipitation driven by drying in the context of CO_2 injection. Energy Procedia 4, 4387–4394.

Prasianakis, N.I., Curti., E., Kosakowski, G., Poonoosamy, J., Churakov, S.V., 2017. Deciphering pore-level precipitation mechanisms. Scientific Reports 7, 13765.

Preuss, k. and Zhang, K., 2008. Numerical modeling studies of the dissolution-diffusion-convection process during CO_2 storage in saline aquifers. Technical Report LBNL-1243E, Lawrence Berkeley National Laboratory, Berkeley, California, USA. 33 p.

Pruess, K., Müller, N., 2009. Formation dry-out from CO_2 injection into saline aquifers: 1. Effects of solids precipitation and their mitigation. Water Resources Research 45 (3), W03402.

Pudlo, D., Henkel, S., Reitenbach, V., Albrecht, D., Enzmann, F., Heister, K., Pronk, G., Ganzer, L., Gaupp, R., 2015. The chemical dissolution and physical migration of minerals induced during CO_2 laboratory experiments: their relevance for reservoir quality. Environ. Earth Sci. 73, 7029–7042.

Ramm, M., Forsberg, A.W., Jahren, J.S., 1997. Porosity–depth trends in deeply buried Upper Jurassic reservoirs in the Norwegian Central Graben: an example of porosity preservation beneath the normal economic basement by grain-coating microquartz. In: Kupecz, J.A., Gluyas, J., Bloch, S. (eds): Reservoir quality prediction in sandstones and carbonates. AAPG Memoir 69, 177–199.

Raoof, A., Nick, H.M., Wolterbeek, T.K.T., Spiers, C.J., 2012. Pore-scale modeling of reactive transport in wellbore cement under CO2 storage conditions. International Journal of Greenhouse Gas Control 11S, S67–S77.

Rasmussen, E.S., Laghari, S., 2020. Capture, Storage and Use of CO_2 (CCUS): Seismic interpretation of existing 2D seismic data around the Hanstholm structure (Part of work package 5 in the CCUS project). Geological Survey of Denmark and Greenland report 2020/45, 26 pp.

Rosenbrand, E., C. Kjøller, J. F. Riis, F. Kets and I. L. Fabricius (2015). Different effects of temperature and salinity on permeability reduction by fines migration in Berea sandstone. Geothermics 53(0): 225-235.

Rosenbrand, E., Haugwitz, C., Jacobsen P.S.M., Kjøller, C., Fabricius, I.L., 2014. The effect of hot water injection on sandstone permeability. Geothermics 50, 155–166.

Saint-Garcia, A., Abarca, E., Nardi, A., Grandia, F., Oelkers, E. H. (2017) Convective mixing fingers and chemistry interaction in carbon storage. International Journal of Greenhouse Gas Control 58, 52–61.

Sayegh, S.G., Krause, F.F., Girard, M., DeBree, C., 1990. Rock/fluid interactions of carbonated brines in a sandstone reservoir: Pembina Cardium, Alberta, Canada. SPE Formation Evaluation 5, 399–405.

Sbai, M.A., Azaroual, M., 2011. Numerical modeling of formation damage by two-phase particulate transport processes during CO_2 injection in deep heterogeneous porous media. Advances in Water Resources 34, 62–82.

Scheibe, T.D., Schuchardt, K., Agarwal, K., Chase, J., Yang, X., Palmer, B.J., Tartakovsky, A.M., Elsethagen, T., Redden, G., 2015. Hybrid multiscale simulation of a mixing-controlled reaction. Advances in Water Resources 83, 228-239.

Sharma, Mukul M., Pang, Shutong, Wennberg, K.E., Morgenthaler, L.N., 2000. Injectivity decline in water-injection wells: an offshore Gulf of Mexico case study.

Silverstri, A., Budi., A., Ataman, E., Olsson., M.H.M., Andersson, M.P., Stipp, S.L.S., Gale, J.D., Raiteri, P., 2017. A quantum mechanically derived force field to predict CO_2 adsorption on calcite. Journal of Physical Chemistry C 121, 24025-24035.

Sin and Corvisier (2019) Multiphase multicomponent reactive transport and flow modeling. Reviews in Mineralogy Geochemistry 85, 143-195.

Sokama-Neuyam, Y., Ursin, J., 2015. The Effect of Mineral Deposition on CO_2 Well Injectivity. EUROPEC. Society of Petroleum Engineers.

Sokama-Neuyam, Y.A., Ginting, P.U.R., Timilsina, B., Ursin, J.R., 2017. The impact of fines mobilization on CO_2 injectivity: an experimental study. International Journal of Greenhouse Gas Control 65, 195–202.

Springer, S., Dideriksen, K., Holmslykke, H.D., Kjøller, C., Olivarius, M., Schovsbo, N., 2020. Capture, Storage and Use of CO_2 (CCUS): Seal capacity and geochemical modelling (Part of work package 5 in the CCUS project). Geological Survey of Denmark and Greenland report 2020/30, 42 pp.

Spycher, N.F., Llanos, E.M., Vu, H.P., Haese, R.R., 2019. Reservoir scale reactive-transport modeling of a buoyancy-controlled CO_2 plume with impurities (SO_2, NO_2, O_2). International Journal of Greenhouse Gas Control 89, 40–51.

Steefel, C.I., Molins, S., Trebotich, D., 2013. Pore scale processes associated with subsurface CO_2 injection and sequestration. Reviews in Mineralogy Geochemistry 77, 259-303.

Sundal, A., Hellevang, H., 2019. Using reservoir geology and petrographic observations to improve CO_2 mineralization estimates: Examples from the Johansen Formation, North Sea, Norway. Minerals 9, 671.

Taheri, A., Lindeberg, E., Torsæter, O., Wessel-Berg, D., 2017. Qualitative and quantitative experimental study of convective mixing process during storage of CO_2 in homogeneous saline aquifers. International Journal of Greenhouse Gas Control 66, 159-176.

Takenouchi S, Kennedy GC. 1964. The binary system H_2O-CO_2 at high temperatures and pressures. American Journal of Science 262,1055-1074

Takenouchi S, Kennedy GC, 1965. The solubility of carbon dioxide in NaCl solutions at high temperatures and pressures. American Journal of Science 263, 445-454

Tang, Y., Lv, C., Wang, R., Cui, M., 2016. Mineral dissolution and mobilization during CO_2 injection into the water-flooded layer of the Pucheng Oilfield, China. Journal of Natural Gas Science and Engineering 33, 1364–1373.

Tokada, N., Xu, T., 2017. Reactive transport simulation to assess geochemical impact of impurities. International Journal of Greenhouse Gas Control 66, 177–189.

Torsæter, M., Cerasi P., 2018. Geological and geomechanical factors impacting loss of near-well permeability during CO_2 injection. International Journal of Greenhouse Gas Control 76, 193-199.

Varloteaux, C., Békri, S., Adler, P.M., 2013. Pore network modelling to determine the transport properties in presence of a reactive fluid- From pore to reservoir scale. Advances in Water Resources 53, 87–100.

Vejbæk, O.V., 1997. Dybe strukturer i danske sedimentære bassiner. Geologisk Tidsskrift 4, 1–31.

Venkitaraman, A., Roberts, P.M., Sharma, M.M., 1995. Ultrasonic Removal of Near-Wellbore Damage Caused by Fines and Mud Solids. SPE Drilling & Completion 10. SPE-27388-PA

Vilarrasa, V., Silva, O., Carrera, J., Olivella, S., 2013. Liquid CO_2 injection for geological storage in deep saline aquifers. International Journal of Greenhouse Gas Control 14, 84–96.

Vosgerau, H., Gregersen, U., Hjuler, M.L., Holmslykke, H.D., Kristensen, L., Lindström, S., Mathiesen, A., Nielsen, C.M., Olivarius, M., Pedersen, G.K., Nielsen, L.H., 2016a. Reservoir prognosis of the Gassum Formation and the Karlebo Member within two areas of interest in northern Copenhagen. The EUDP project "Geothermal pilot hole, phase 1b". Geological Survey of Denmark and Greenland report 2016/56, 138 pp.

Vosgerau, H., Gregersen, U., Kristensen, L., Lindström, S., Mathiesen, A., Nielsen, C.M., Olivarius, M., Nielsen, L.H., 2017. Towards a geothermal exploration well in the Gassum Formation in Copenhagen. Geological Survey of Denmark and Greenland Bulletin 38, 29–32.

Vosgerau, H., Gregersen, U., Laghari, S., 2020. Capture, Storage and Use of CO_2 (CCUS): Seismic interpretation of existing 3D seismic data around the Stenlille structure within the framework of sequence stratigraphy and with focus on the Gassum Formation (Part of Work package 6 in the CCUS project). Geological Survey of Denmark and Greenland report 2020/34, 53 pp.

Vosgerau, H., Mathiesen, A., Andersen, M.S., Boldreel, L.O., Hjuler, M.L. Kamla, E., Kristensen, L., Pedersen, C.B., Pjetursson, B., Nielsen, L.H., 2016b. A WebGIS portal for exploration of deep geothermal energy based on geological and geophysical data. Geological Survey of Denmark and Greenland Bulletin 35, 23–26.

Vosgerau, H., Mathiesen, A., Kristensen, L., Andersen, M.S., Hjuler, M.L., Laier, T., 2015a. Det geotermiske screeningsprojekt. Kalundborg-lokaliteten. Geological Survey og Denmark and Greenland report 2015/53, 35 pp.

Vosgerau, H., Mathiesen, A., Kristensen, L., Andersen, M.S., Hjuler, M.L., Laier, T., 2015b. Det geotermiske screeningsprojekt. Thisted-lokaliteten. Geological Survey og Denmark and Greenland report 2015/47, 31 pp.

Wallace, A.F., Hedges, L.O., Fernandez-Martinez, A., Raiteri, P., Gale, J.D., Waychunas, G.A., Whitelam, S., Banfield, JF., De Yoreo, J.J., 2013. Microscopic evidence for liquid-liquid separation in supersaturated $CaCO_3$ solutions. Science 885-889.

Weibel, R., Kjøller, C., Bateman, K., Laier, T., Nielsen, L.H., Purser, G., 2014. Carbonate dissolution in Mesozoic sand- and claystones as a response to CO_2 exposure at 70 °C and 20 MPa. Applied Geochemistry 42, 1-15.

Weibel, R., Olivarius, M., Kristensen, L., Friis, H., Hjuler, M.L., Kjøller, C., Mathiesen, A., Nielsen, L.H., 2017a. Predicting permeability of low-enthalpy geothermal reservoirs: A case study from the Upper Triassic − Lower Jurassic Gassum Formation, Norwegian–Danish Basin. Geothermics 65, 135–157.

Weibel, R., Olivarius, M., Kjøller, C., Kristensen, L., Hjuler, M.L., Friis, H., Pedersen, P.K., Boyce, A., Andersen, M.S., Kamla, E., Boldreel, L.O., Mathiesen, A., Nielsen, L.H., 2017b. The influence of climate on early and burial diagenesis of Triassic and Jurassic sandstones from the Norwegian–Danish Basin. The Depositional Record 3(1), 60–91.

Weibel, R., Olivarius, M., Vosgerau, H., Mathiesen, A., Kristensen L., Nielsen, C.M., Nielsen, L.H., 2020. Overview of potential geothermal reservoirs in Denmark. Netherlands Journal of Geosciences 99, e3, 14 pp.

Wilkinson, M., Haszeldine, R.S., Fallick, A.E., Odling, N., Stoker, S.J., Gatliff, R.W., 2009. CO_2-mineral reaction in a natural analogue for CO_2 storage--Implications for modeling. Journal of Sedimentary Research 79, 486–494.

Xie, Q, Saeedi A., Piane, C. D., Esteban L., Brady P. V. (2017) Fines migration during CO_2 injection: experimental results interpreted using surface forces. International Journal of Greenhouse Gas Control 65, 32-39.

Xiong, Q., Baychev, T.G., Jivkov, A.P., 2016. Review of pore network modelling of porous media- Experimental characterisations, network constructions and applications to reactive transport. Journal of Contaminant Hydrology 192, 101–117.

Xu, T., Apps, J.A.,Pruess, K., Yamamoto, H., 2007. Numerical modeling of injection and mineral trapping of CO_2 with H_2S and SO_2 in a sandstone formation. Chemical Geology. 242, 319–346.

Xu, T., Spycher, N., Sonnenthal, E., Zhang, G., Zheng, L., Pruess, K., 2011. TOUGHREACT Version 2.0: A simulator for subsurface reactive transport under non-isothermal multiphase flow conditions. Computers and Geosciences. 37, 763–774.

Appendix 1

Methods for 1D reactive transport calculations

In the 1D reactive transport modelling conducted with PHREEQC and its native database, the temperature was set to 80 °C and the pressure, to 100 atm. Each cell contained 1 kg water and the corresponding amount of minerals based on a porosity of 20% and a volumetric abundance of 79% for quartz, 5% for calcite, 3% for siderite, 3% for muscovite, 5% for oligoclase and 5% for K-feldspar based roughly on mineralogical characterisation of the Gassum formation. The formation water before CO_2 injections was assumed to have a pH of 6.4, be rich in Na and Cl and have equilibrated with calcite, siderite, quartz, muscovite, kaolinite and CO_2 with a partial pressure of 10^{-2}. The resulting formation water is given in table A1.

Of the primary minerals, calcite, siderite and muscovite were assumed to be in equilibrium with the solution at all times to limit computational time. For calcite and siderite, simpler calculations showed that equilibration occurred practically instantaneous, consistent with calcite dissolution rates being controlled by the rate of transport of reactants and products from the mineral water interface at the conditions. Modelling of the diffusion of the reactants and products within a 0.2 mm pore, indicated that the water in the pore reached equilibrium within 1 hour. Thus, the assumption about equilibrium in the calculations seems very reasonable for the carbonates, which constitute a considerable fraction of the minerals in the Gassum formation.

For Oligoclase and K-feldspar, the extend of dissolution were assumed to be controlled by reaction kinetics using Equations KD1 to KD5 and the data compiled by Palandri and Kharaka (2004). In the calculation of dissolution rates, the surface area was assumed to be that of a sphere with a diameter of 0.5 mm for feldspar. The surface area was not corrected for the decrease in surface area that occurs as dissolution cause grains to diminish in size. Quarts was considered unable to grow because of the relatively low temperature. Consequently, the secondary phases allowed to form during the reaction included amorphous silica ($SiO_{2(a)}$), calcite, siderite, muscovite, kaolinite. These phases were assumed to form instantly upon exceeding solubility. PHREEQC only features solubility products for the pure plagioclase endmembers, albite and anorthite. Consequently, the solubility for oligoclase was determined assuming ideal solid solution (Annórsson and Stefánsson 1999). Table A2 gives an overview of the values of the parameters used in the calculation.

Table A1. Composition of formation water assumed in the calculations in moles per kg water. DIC refers to total dissolved inorganic carbon.

Element	Moles/kgw
Al	$6*10^{-7}$
Ca	0.2
Cl	1.4
Fe(II)	$2.2*10^{-3}$
K	$2.8*10^{-6}$
Na	1.0
Si	$2.3*10^{-4}$
DIC	$5.3*10^{-3}$
pH	6.4

Table A2. Solid phases and their parameters used in the PHREEQC 1D reactive transport modelling.

	Calcite	**Siderite**	**Kaolinite**	**Muscovite**	**SiO_2(a)**	**Oligoclase**	**K-Feldspar**
Formula	$CaCO_3$	$FeCO_3$	$Al_2Si_2O_5(OH)_4$	$KAl_3Si_3O_{10}(OH)_2$	SiO_2	$Na_{0.8}Ca_{0.2}Al_{1.2}Si_{2.8}O_8$	$KAlSi_3O_8$
Abundance (vol%)	5%	3%	0%	3%	0%	5%	5%
Molar volume (cm^3/mol)	36.9	29.2	99.35	29	141.21	102.06	108.15
Reaction type	---------- Equilibrium ----------					Kinetic	Kinetic
log Ksp (80 °C; 100 atm)	-8.91	-11.1	3.5	5.87	-2.35	-15.7	-16.91
A_a						$10^{-9.67}$	$10^{-10.06}$
A_n						$10^{-11.84}$	$10^{-12.41}$
$E_{a(a)}$						65	51.7
$E_{a(n)}$						69.8	38.0
n						0.457	0.5